atmosphere

MDPI

Article

Assessing Urban Flood Hazard Vulnerability Using Multi-Criteria Decision Making and Geospatial Techniques in Nabadwip Municipality, West Bengal in India

Tanmoy Basu [1], Biraj Kanti Mondal [2,*], Kamal Abdelrahman [3], Mohammed S. Fnais [3] and Sarbeswar Praharaj [4]

[1] Faculty (SACT-1), Department of Geography, Katwa College, Katwa 713130, West Bengal, India; tanmoybasu.2017@gmail.com
[2] Department of Geography, Netaji Subhas Open University, Kolkata 700064, West Bengal, India
[3] Department of Geology and Geophysics, College of Science, King Saud University, Riyadh 11451, Saudi Arabia
[4] Knowledge Exchange for Resilience, School of Geographical Sciences and Urban Planning, Arizona State University, Tempe, AZ 85281, USA
* Correspondence: birajmondal.kolkata@gmail.com; Tel.: +91-8240506428

Abstract: The flood hazard risks and vulnerability in the urban areas alongside major rivers of India have been gradually increasing due to extreme climatic events. The present study is intended to assess flood hazard vulnerability and potential risk areas and aims to ascertain the management strategies in Nabadwip Municipality, a statutory urban area of West Bengal. The multi-criteria decision making (MCDM) of selected criteria and geospatial techniques have been employed to determine the urban flood vulnerability in the study area. The study has been conducted using secondary datasets including relevant remotely sensed data and participant observation. The potential flood-affected zones have been determined using the normalized difference flood index (NDFI) and flood vulnerability index (FVI). The analysis of the standardized precipitation index (SPI) of 20 years of monthly precipitation shows the variability of seasonal rainfall distribution in the study area. Furthermore, the spatial distribution of the composite Ibrahim index of socio-economic development accents that the urban development of the study area was uneven. The municipal wards situated in the central and northeastern portions of Nabadwip Municipality were extremely vulnerable, whereas the western and southwestern wards were less vulnerable. It is also revealed from the strengths–weaknesses–opportunities–challenges (SWOC) of the principal management strategies of the flood situation analysis that the unplanned sewerage system is one of the most effective weaknesses in the area. All-embracing and integrative flood management strategies need to be implemented in the study area considering the intra-regional vulnerability and development for the resilient and sustainable development of the study area.

Keywords: urban flood; vulnerability; MCDM; SWOC; NDFI; FVI; integrated management

Citation: Basu, T.; Mondal, B.K.; Abdelrahman, K.; Fnais, M.S.; Praharaj, S. Assessing Urban Flood Hazard Vulnerability Using Multi-Criteria Decision Making and Geospatial Techniques in Nabadwip Municipality, West Bengal in India. *Atmosphere* **2023**, *14*, 669. https://doi.org/10.3390/atmos14040669

Academic Editor: Ognjen Bonacci

Received: 7 February 2023
Revised: 21 March 2023
Accepted: 27 March 2023
Published: 31 March 2023

1. Introduction

Flood occurrences and their consequences present a challenging circumstance for urban dwellers worldwide, particularly in developing countries [1]. Several urban residents in newly developed flood-prone areas in developing countries are at risk of flooding as a result of rising urbanization and population growth [1]. The frequency and intensity of urban floods are influenced by many indicators. Urban areas' flood vulnerability and risk are driven by the topography and several socio-economic indicators that are related to flood 'exposure', 'sensitivity', and 'adaptive capacity' [2]. In the era of climate change, human-induced activities and rapid urbanization are worsening the risk of flood vulnerability [1]. At present, climate change can transform the conditions of precipitation, which

changes the nature, extent, and affectivity of floods [3]. This is exemplified by the fact that a devastating flood occurred in the Chao Phraya and Mekong River basins of Thailand due to the heavy rainfall during the monsoon season in 2011 [3]. The projection of urban flooding indicated an increasing trend from 2020 to 2040 in the Hohhot region of Mongolia, China [4]. The two interrelated aspects of vulnerability are 'economic development' and 'urban flooding' [5]. Economic prosperity in urban areas without any deliberate urban development negatively impacted the recurrent causes of flooding [5]. Bangladesh, China, and Vietnam are frequently at risk of flooding because of the intense monsoon rains [5]. The largest flood-prone countries in the world are China, India, the United States, and Indonesia [6]. Human activities in the planning and development of cities have a significant impact on flood incidents [6]. Financial damage and the threat to human lives are the most disastrous effects of floods in urban areas [6]. In this context, previous literature has been thoroughly reviewed to conceptualize the nature, scope, indicators, vulnerability, and resilience of urban floods. One of the most catastrophic natural and man-made disasters is flooding [7]. The natural land surface was converted into built-up areas as a result of the rising population, which increased the frequency of floods in urban areas and impaired 3.6 million people between 2010 and 2020 [7]. Assessment of flood risk and vulnerability in Mexico has been researched in the context of climate change [8]. In Nan Province of Thailand, where the elevation is low near the river, the municipal area has experienced the majority of the floods [9]. Urban amenities, employment, supply chains, and urban infrastructure in Bangladesh and Nepal have all been severely impacted due to flood incidents [10]. In India, numerous floods had an impact on city dwellers' livelihoods. Major Indian cities had been impacted by flood hazards and associated vulnerabilities. The major urban flood incidents in India occurred in Hyderabad (2000), Kolkata (2007), Delhi (2010), Chennai (2015), and Mumbai (2017) [11–13]. The research presented in [13] revealed the environmental and human-caused causes of urban flooding. Urban floods in India are primarily caused by extreme rainfall conditions, powerful thunderstorms, river course changes, and river bank erosion [13]. Deforestation, the concretization of the ground's surface, and the encroachment of floodplains by rapidly expanding built-up areas were the main anthropogenic factors [13]. Other anthropogenic factors included poor drainage channel management, heavy water discharge from check dams, and a lack of preparedness for disasters [13]. Using the multi-criteria decision making method, several factors have been integrated to assess urban flood vulnerability. According to the definition of vulnerability given in the study [14], vulnerability is a potential risk measurement strategy that incorporates socio-economic factors to build disaster preparedness. Digital elevation models (DEMs), soil, rainfall, slope, drainage density, and land use and land cover (LULC) are among the common physical factors used by researchers [14–18]. Other physical factors include the following: topographic wetness index (TWI), normalized difference vegetation index (NDVI), modified normalized difference water index (MNDWI), normalized difference built-up index (NDBI), distance from the river, stream power index, and sediment transport index (STI) [14–18]. An established Multi-Criteria Decision Making (MCDM) technique for creating a flood vulnerability index with the integration of geoinformatics is the analytical hierarchy process (AHP). In Kanyakumari, India, flood vulnerability was assessed using AHP [14]. The AHP method was used to analyze the flash flood susceptibility in Bangladesh's northeast wetland [15]. To determine the flood risk and vulnerability in the Tapi River basin in India, integrated AHP and geographic information system (GIS) methods were applied [17]. To determine the degree of flood vulnerability in the Indian Western Ghat foothills, a comparison of the AHP and fuzzy-AHP methods was introduced [18]. To determine flood vulnerability in the Indian district of Ernakulam, the methodological prediction of the AHP and Fuzzy Analytical Hierarchy Process (F-AHP) methods was also assessed [16]. Different socio-economic factors related to flood vulnerability identified in [18] were the total population, the number of households, the literacy rate, and the Scheduled Castes and Scheduled Tribes population in the foothill areas of the Western Ghat in India. The study [19], at Nabadwip Municipality in West

Bengal, India, identified various urban amenities associated with flood conditions. West Bengal experienced significant urban floods in 1956, 1959, 1978, 1995, 1999, and 2000 as a result of heavy rainfall and high discharge in September and October [20]. A large number of populations in West Bengal were adversely affected by the flood in 2000 for an extended period due to inadequate management and a lack of planning and control structures [20]. Several damages and vulnerabilities are the major consequences of floods in Indian cities. There was a connection between urbanization and the frequency of floods. According to [21], flood risks in Nigeria's Gombe metropolis significantly increased as drainage infrastructure deteriorated. In Shanghai, China, urban forestry significantly reduced flood conditions caused by substantial rainfall [22]. In-depth planning is required to lessen the flood vulnerability in urban areas. To reduce the risks of urban flooding in Indian cities, strategic protection of river 'catchment' areas, enhancement of 'water disposal systems', land-use planning, 'flood vulnerability mapping', 'watershed management', and construction of 'flood walls' are usually required [13]. The establishment of 'relief centers' and early warning and recovery systems for floods are also part of the strategic planning and policies for mitigating and managing the effects of floods in Indian cities [23].

The present study has been conducted in the context of changing flood vulnerability and related factors in the study area. Based on the literature review and associated field observations, the study includes a framework of the trend of flood hazards and their relationship with urban development in the study area. The present study develops a comprehensive appraisal of flood hazard vulnerability in the study area based on prior research on the flood hazards of developing countries such as India (particularly the state of West Bengal). Table 1 outlines the relevant literature that pertains to the contextual background of the study, such as analytical approaches to urban flooding, assessments of flood vulnerability, scenarios and occurrences of urban flood hazards in India and West Bengal, the relationship between flood vulnerability and urban development, and flood adaptation and resilience.

The concept of flood vulnerability, its relationship to climate change, flood contributing factors, the nature of geographical expansion efficacy, and mitigation measures for floods have all been separately explored in the previous literature. However, an integrated study is required to identify the physical factors of flood vulnerability and its occurrences in a region where rainfall varies seasonally. Additionally, a correlation between the flood vulnerability factors and the normalized difference flood index has to be established. Understanding the connection between urban development and flood vulnerability is imperative to find out how to assess flood mitigation strategies in urban areas using a strengths–weaknesses–opportunities–challenges analysis. The unique aspect of the present study is the use of physical and environmental factors to determine the flood vulnerability index and compare this index to the socio-economic development of the study area. Additionally, the study measures the predicted value of the flood-related spectral index. A significant aspect of managing quasi-natural disasters is measuring flood vulnerability by considering the interconnection between physical and socio-economic factors. The study also highlights the challenges faced by the locals as a result of flood events, and it acts accordingly to mitigate floods as well as provide better opportunities for the livelihood of the urban dwellers. In this context, the aims of the present study are as follows:

1. To identify the physical and environmental factors of flood hazard in the study area in 2000 and 2015;
2. To delineate the flood vulnerability zones in the study area in 2000 and 2015;
3. To analyze the relationship between flood vulnerability and urban development;
4. To measure a flood mitigation strategy using strengths–weaknesses–opportunities–challenges analysis.

Table 1. Literature regarding the conceptual background of the study.

Conceptual Background	Literature Review	Sources
Analytical approaches to urban flooding and the assessment of vulnerability	The focus of current research is on measuring flood risk in urban areas around the world using remote sensing and GIS. Analytical hierarchy processes with geographic information systems are one of the methods most frequently used to assess flood hazard vulnerability.	[24,25]
Urban flood scenarios in India	The urban areas were severely impacted by large urban floods that were primarily raised by heavy rain in Mumbai (on 26 July 2005), Kolkata (30 June 2007), and Chennai (in November and December 2015).	[26]
Studies on flood occurrences in West Bengal	West Bengal has annual flood potential areas that constitute 29.84% of the state's total geographical area. Bardhhaman (undivided), Birbhum, Murshidabad, Nadia, Hugli, and Midnapore (undivided) were the major flood-prone areas of West Bengal.	[27]
Flood vulnerability assessment in West Bengal	Studies using remote sensing data and GIS analysis revealed that the districts of Nadia and Bardhaman contained a high concentration of settlements that were extremely susceptible to flooding from 1991 to 2000. According to the micro-level administrative scale, Nabadwip in the Nadia district was situated in a high-severity hazard-prone zone in Gangetic West Bengal.	[28,29]
Determinants of vulnerability and adaptation to floods in West Bengal	In the Murshidabad district of West Bengal, one of the main border districts of Nadia, significant household-level determinants predicted livelihood vulnerability based on exposure to flood sensitivity and adaptive capacity.	[30]
Urban development and flood disaster in Kolkata	The risks of flooding in Kolkata, the capital of West Bengal, have increased as a result of the legacy of poor planning and an uneven distribution of geographic elements.	[31]
Flood occurrences in Nadia district in West Bengal	Over the past few years, the district of Nadia has experienced major floods (1995–2000). According to a report from 20 August 2015, the flood incident had an impact on 21,508 residents of Nabadwip city. The majority of them were engaged in agriculture and household industries.	[32]
Flood resilience in West Bengal	A comprehensive and well-developed plan for flood recovery needs to be implemented while focusing on the flood mitigation strategies in West Bengal.	[33]

Source: A literature review by the authors.

2. Hypothesis

Based on the conceptual background of flood vulnerability analysis, the present study establishes a hypothesis as follows:

Null Hypothesis (H_0). *There is no significant relationship between flood vulnerability and urban development in the study area.*

Alternative Hypothesis (H_1). *There is a significant negative relationship between flood vulnerability and urban development in the study area.*

The study tends to reject the statement that there is no significant relationship between flood vulnerability and urban development in the study area to establish a research hypothesis. Details of methods of hypothesis testing are discussed in Section 3.4.

3. Materials and Methods

3.1. Study Area

Nabadwip Municipality, a statutory town of Nadia district in West Bengal, India, has been selected as the study area. The urban area is situated between 23 degrees 2 min north and 23 degrees 23 min north latitude and 88 degrees 2 min east and 88 degrees 23 min east longitude [19]. The municipality area is situated on the western bank of the river Bhagirathi-Hugli, and its elevation above mean sea level (M.S.L.) is 18 m (59.0551 feet) [19]. The area is a part of the mature delta of the Bhagirathi-Hugli River plain, which formed a slope from north to south. The surrounding floodplain areas are characterized by braided river channels, meandering, sand bars, oxbow lakes, and scattered water bodies [34]. Nabadwip

Municipality is located in the region of India with a tropical monsoon climate, which is typically characterized by significant amounts of rainfall during the monsoon season. Based on the field observation, it was determined that the main river channel of Bhagirathi-Hugli is below its normal water-holding capacity, resulting in a high water level during heavy rainfall and surface runoff. This is due to the dredging of water bodies and spill channels for the construction of built-up areas and a large amount of siltation in the river bed due to river bank erosion. Nabadwip Municipality is a Class-I city in India with 24 municipal wards and a population of 125,543 in 2011 [35]. The city is internationally famous for the origin of *Goudiya Vaisnabism*, propounded by *Sri Chaitanya Mahaprabhu* [19]. To examine the dichotomy between urban development and flood vulnerability, the Nabadwip Municipality was selected as the study area. It was noted that during a flood, some of the municipal wards with dense populations and market concentrations close to the city center showed high water levels. The new river course of Bhagirathi-Hugli in the east and the old river course of Bhagirathi-Hugli in the west are the boundaries of the municipality area. In the study area, frequent flood hazards were observed in the late 20th and early 21st centuries. The socio-economic and urban amenity status is properly considered in the present study regarding the impact of flood vulnerability in the municipality area because it is a culturally significant city in West Bengal. Figure 1 shows a representation of the location map and ward map of Nabadwip Municipality.

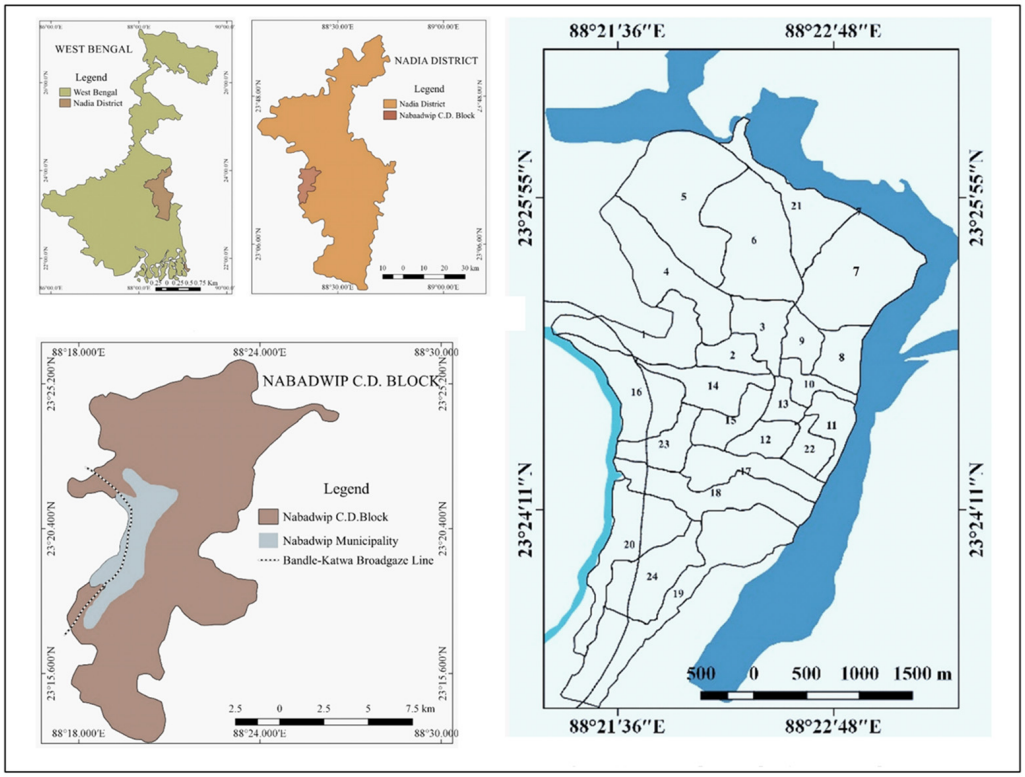

Figure 1. Location map of the study area.

3.2. Data Sources

The study has been conducted using secondary data and field observations. Data have been collected from the Census of India (2011), the Bureau of Applied Economics and Statistics (2015), and the website of Nabadwip Municipality to ascertain the socio-economic conditions and urban amenities in the study area. The website of Solar Radiation Data (SODA), the MERRA Project's collaboration with the National Aeronautics and Space Administration (NASA), has provided daily and monthly rainfall data (January to December of 1986–2016). The National Remote Sensing Center (NRSC) and the United States Geological Survey (USGS) websites were used to gather satellite images from 2000 and 2015. The details of the database and its sources are mentioned in Table 2. Satellite imageries

have been primarily used to develop the spectral indices of flood vulnerability indicators in 2000 and 2015. The monthly rainfall data from 2000 and 2015, the two years in which West Bengal experienced devastating floods, were used to calculate one-month, three-month, four-month, six-month, and twelve-month standardized precipitation indices (SPIs). To determine the long-term variation of precipitation in the study area, a 30-year SPI has also been calculated using the monthly average data from 1986 to 2015. Strengths–weaknesses–opportunities–challenges analysis was implemented after participant observations were accomplished at Nabadwip during the 2015 flood incident to understand the issues arising from the flood and suggest further prospects for the development of the study area.

Table 2. Sources and use of available data.

Sl. No.	Available Data	Date	Source(s)	Methods and Techniques	Web Links
1	(Shuttle Radar Topographic Mission) SRTM-DEM: SRTM1 Arc-Second Global	2 November 2000	[36]	Digital elevation model (DEM), slope analysis, drainage analysis	https://www.earthdata.nasa.gov/sensors/srtm (accessed on 30 August 2022)
2	CARTOSAT DEM (Cartosat-1)	17 April 2015 and 29 April 2015	[37]	Digital elevation model (DEM), slope analysis, drainage analysis	https://bhuvan-app3.nrsc.gov.in/data/download/index.php (accessed on 30 August 2022)
3	LANDSAT ETM^{+} (Enhanced Thematic Mapper Plus)	17 November 2000	[38]	Normalized difference spectral indices	https://earthexplorer.usgs.gov/ (accessed on 30 August 2022)
4	Resourcesat-1/Resourcesat-2: LISS-III (Linear Imaging Self Scanning)	28 November 2015	[39]	Normalized difference spectral indices	https://bhuvan-app3.nrsc.gov.in/data/download/index.php (accessed on 30 August 2022)
5	Rainfall (mm)	1986–2015 (January to December)	[40–42]	Standardized precipitation index	https://mausam.imd.gov.in/ Website of Solar Radiation Data (SODA): Modern-Era Retrospective Analysis for Research and Applications (MERRA) Project collaboration with NASA (https://gmao.gsfc.nasa.gov/reanalysis/MERRA-2/) (accessed on 30 May 2022)

Source: Selected by the authors.

3.3. Research Design

The study's four main segments were designed for the fulfillment of the objectives. Selected indicators of the composite flood vulnerability index have been analyzed using the analytical hierarchy process of multi-criteria decision analysis based on the construction of various spectral indices and the standardized precipitation index. Furthermore, some urban development indicators have been composited using the Ibrahim index of socio-economic development. The correlation–regression model has been used to determine the normalized difference flood index prediction values by the indicators of flood vulnerability and the relationship between the composite flood vulnerability index and the composite Ibrahim index of socio-economic development. Finally, the validation of the composite flood vulnerability index model has been investigated using the reclassification method and the analysis of the area under the receiver operating characteristic curve. The present study also includes hypothesis testing and an analysis of the strengths, weaknesses, opportunities, and threats. Spreadsheets and statistical software were used to develop the mathematical and statistical analyses, as well as the charts and diagrams. The representation of the spatial

distribution of the indices, the zonation map of the composite flood vulnerability index, the composite Ibrahim index, and the area under the receiver operating characteristic curve were all assembled using GIS software. Figure 2 highlights the general methodological framework of the present study.

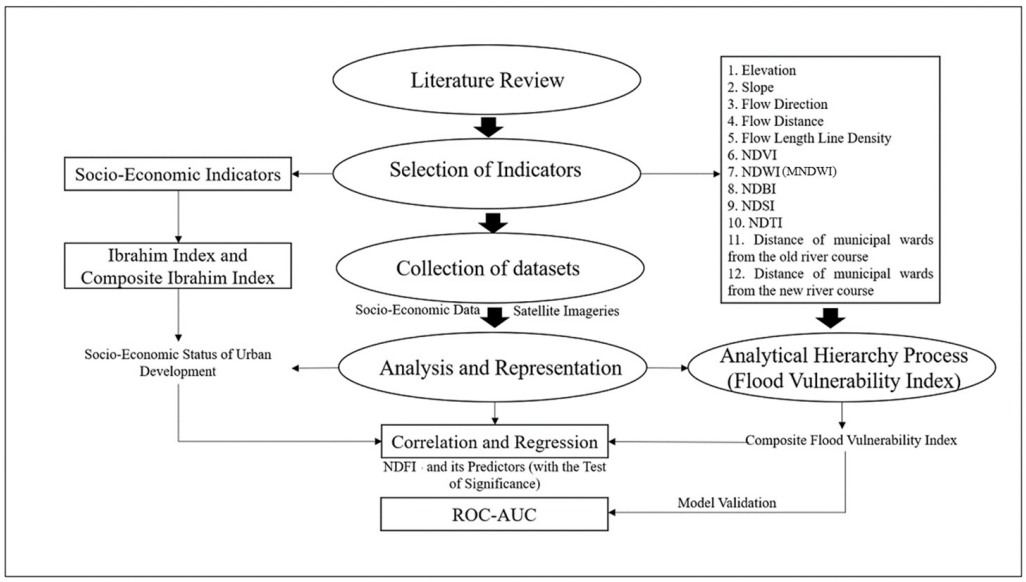

Figure 2. A general methodological framework of the present study.

3.4. Methods and Techniques

3.4.1. Standardized Precipitation Index (SPI) Analysis

The standardized precipitation index is a standardized way to measure anomalies in precipitation [43]. Based on a specific time scale, it indicates the dry or wet state of a region or river basin [44]. SPI has been more consistently analyzed to measure rainfall variability. In [45], SPI was used to measure the spatio-temporal variability of rainfall in China's Fuhe Basin. The Tejo River basin in Portugal underwent an earlier study on flood conditions based on SPI [46]. In the South African city of Durban's eThekwini metropolitan area, SPI was used to evaluate and forecast flood risk [47]. The SPI method had also been used to identify flood risks in Argentina's southern Cordoba Province [48]. The following formula was used to calculate the standardized precipitation index (SPI), which measures precipitation anomalies, using monthly rainfall data (in millimeters (mm); 1 mm = 0.0393701 inches) from the Nabadwip Municipality (1986–2015) based on Krishnagar, the district headquarters of Nadia in West Bengal.

The SPI has been calculated following the formulae [49].

The formula of the mean of the precipitation is

$$Mean(X) = \frac{\sum X}{N} \quad (1)$$

where N is the number of precipitation observations.

The formula for the standard deviation of precipitation is

$$Standard\ Deviation\ (SD) = \sum \sqrt{\frac{\left(X - X\right)}{N}} \quad (2)$$

The skewness of the precipitation has been calculated using the following formula:

$$Skew = \frac{N}{(N-1)(N-2)} \times \sum \left(\frac{X - X}{N}\right) \quad (3)$$

The formulae of conversion of precipitation into lognormal values, Unbiased Statistics (U statistics), and shape and scale parameters of the gamma distribution are as follows:

$$\text{Log mean} = X_{\text{in}} = \text{In}\left(X\right) \tag{4}$$

$$U = X_{\text{in}} \frac{\sum In\ (X)}{N} \tag{5}$$

$$\text{Shape parameter} = \beta = \frac{1 + \sqrt{1 + \frac{4U}{3}}}{4U} \tag{6}$$

$$\text{Scale parameter} = \alpha = \frac{X}{\beta} \tag{7}$$

The cumulative probability of an observed precipitation event has been calculated by using the output parameters [50]. The cumulative probability is calculated by

$$G\ (x) = \frac{\int_0^x x^{a-1} e^{\frac{-x}{\beta}}\ dx}{\beta^a\ \Gamma(a)} \tag{8}$$

The formula for the calculation of cumulative probability is

$$H\ (x) = q + (1-q)\ G\ (x) \tag{9}$$

where q is the probability of zero.

When the gamma function is undefined for $x = 0$ and a precipitation distribution may contain zeros [50], the SPI values are calculated following [49] the transformation of the cumulative probability $H\ (x)$ into the standard normal random variable Z with a mean of 0 and variance of 1 [50]. An alternative equation of the approximate conversion [51] is

$$Z = SPI = -\left(t - \frac{c_0 + c_1 t + c_2\ t^2}{1 + d_1 t + d_2 t^2 + d_3 t^3}\right) 0 < H(x) \leq 0.5 \tag{10}$$

$$Z = \text{SPI} = -\left(t - \frac{c_0 + c_1 t + c_2\ t^2}{1 + d_1 t + d_2 t^2 + d_3 t^3}\right) 0.5 < H(x) \leq 1 \tag{11}$$

where

$t = \sqrt{in\left(\frac{1}{H(x)^2}\right)} 0 < H(x) \leq 0.5;$

$t = \sqrt{in\left[\frac{1}{\{1.0 - H(x)\}^2}\right]} 0.5 < H(x) \leq 1.0;$

$c_0 = 2.515517;$

$c_1 = 0.802583;$

$c_2 = 0.010328;$

$d_1 = 1.432788;$

$d_2 = 0.189269;$

$d_3 = 0.001308.$

In Equations (10) and (11), the values of c_0, c_1, c_2, d_1, d_2, and d_3 are constants that are extensively used to enumerate SPI [51].

Thus, SPI values that indicate the four categories of drought [52] are I, Mild Drought; II, Moderate Drought; III, Severe Drought; and IV, Extreme Drought.

3.4.2. Digital Elevation Model (DEM) and Raster Analyses

Layouts for DEM and raster analyses of the selected flood vulnerability indicators have been prepared using geoinformatics. The DEM analysis has measured the relief in meters (1 m = 3.28084 feet), slope in percentage, flow direction, length, and density of the flow length lines. Spectral indices, such as the normalized difference vegetation index (NDVI), the normalized difference water index (NDWI), the modified normalized difference water index (MNDWI), the normalized difference built-up index (NDBI), the normalized difference flood index 2 (NDFI2), the normalized difference turbidity index (NDTI), and the normalized difference soil index (NDSI), have been measured using raster analysis of extracted band compositions of satellite images. The details of the formulae are mentioned in Table 3.

Table 3. Details of the parameters and indicators used in the present study.

Indicators	Measurement	Source(s)	Justification for Selection
Standardized Precipitation Index (SPI)	The detailed formula has been mentioned in the Section 3.	[49]	Standardized precipitation index for analyzing monthly/annual drought conditions.
Relief (R) in m (1 m = 3.28084 feet)	Derived from Digital Elevation Model (DEM)	[53,54]	Terrain analysis and relief aspect of the morphometry of drainage basin.
Slope (S) in %	$S = (Z \times (Ctl/H))/(10 \times A)$, basin area ($A$), total basin relief ($H$), the maximum height of the basin (Z) and total contour length, the average angle of slope ($tan\tilde{O}$) = Average No. of contour crossings per mile (A) × contour interval (I) 3361 (constant)	[55]	Terrain analysis and relief aspect of the morphometry of drainage basin.
Flow direction (Fdir)	Derived from DEM	[56,57]	The linear aspect of the flow of the drainage basin.
Flow distance (Fdist) in km (0.621371 miles)	Derived from DEM	Spatial analyst in GIS	The linear aspect of the flow of the drainage basin.
Flow length in km (Fl) (0.621371 miles)	Derived from stream raster	[56]	The linear aspect of the flow of the drainage basin.
Flow length line density (Fld) in km/square km (0.621371 mile/ 0.38610191964 square mile)	Derived from stream raster using line density feature in GIS analysis	Spatial analyst in GIS	The areal aspect of the flow of the drainage basin.
Normalized Difference Vegetation Index (NDVI)	$NDVI = \frac{NIR\ (Near\ Infrared) - RED}{NIR(Near\ Infrared) + RED}$	[58]	Satellite imagery-based spectral index of vegetation conditions.
Normalized Difference Water Index (NDWI)	$NDWI = \frac{Green - NIR}{Green + NIR}$	[59]	Satellite imagery-based spectral index of surface water conditions.
Modified Normalized Difference Water Index (MNDWI)	$MNDWI = \frac{Green - SWIR}{Green + SWIR}$	[60]	Satellite imagery-based spectral index of surface water conditions.
Normalized Difference Built-Up Index (NDBI)	$NDBI = \frac{SWIR - NIR}{SWIR + NIR}$	[61]	Satellite imagery-based spectral index of habitation conditions.
Normalized Difference Turbidity Index (NDTI)	$NDTI = \frac{Red - Green}{Red + Green}$	[62,63]	Satellite imagery-based spectral index of the relative clarity conditions of rivers.

Table 3. *Cont.*

Indicators	Measurement	Source(s)	Justification for Selection
Normalized Difference Soil Index (NDSI)	$NDSI = \frac{(Band7-Band2)}{(Band7+Band2)}$ (For ETM$^+$ Band7 = SWIR2 and Band2 = Green.)	[64]	Satellite imagery-based spectral index of soil conditions.
Normalized Difference Flood Index 3 ($NDFI_2$)	$NDFI_2 = \frac{Red-SWIR}{Red+SWIR}$	[65–67]	Satellite imagery-based spectral index of flood conditions.
Normalized Difference Flood Index 3 ($NDFI_3$)	$NDFI_3 = \frac{Blue-SWIR\_2}{Blue+SWIR\_2}$	[65,67]	Satellite imagery-based spectral index of flood conditions.

Source: Selected by the authors.

The normalized difference flood index is one of the significant spectral index measurements. In the aftermath of the floods in Malaysia's Kelantan Province in December 2014, land use estimation was directed using NDFI3 [65]. The Piemonte–Lombardia regions of Italy, the West Godavari of India, the Mekong Delta of Vietnam, and Siem Reap in Cambodia all had flood conditions that were analyzed using NDFI1 and NDFI2 [66]. Using Earth observation datasets, the construction of the NDFI was used to map the flooded areas in Southern Malawi (2015); Veneto, Italy (2010); and Northern Uganda (2015) [67]. Concerning this, the following formula has been used to calculate the normalized difference flood index 2 (NDFI2) and normalized difference flood index 3 (NDFI3) [65,67].

$$NDFI_2 \quad \frac{Red - SWIR}{Red + SWIR} \tag{12}$$

$$\text{and } NDFI_3 \quad \frac{Blue - SWIR\_2}{Blue + SWIR\_2} \tag{13}$$

where *SWIR* is shortwave infrared.

3.4.3. Flood Vulnerability Index (FVI)

The analytical hierarchy process (AHP), a method of statistical decision making under the multi-criteria decision making (MCDM) process, has been used to calculate a statistical measure of the flood vulnerability index (FVI). The previous studies [68,69] used this method to calculate the flood vulnerability index. Measurement based on "the dependence within and between the group of the elements" is the analytical hierarchy process [70]. There are four steps combined to complete the entire process. The following are the subsequent steps:

First, the hierarchy of the criteria, sub-criteria, attributes, and decision alternatives is derived [71]. Second, a 9-point scale measuring preference for the pairwise comparison of individual criteria based on [72] is constructed. The formulation of the pairwise comparison matrix, $A = \left[a_{ij}\right]_{n\times n}$ is written as

$$A = \begin{bmatrix} a_{11} & a_{12} & \cdots & \cdots & a_{1n} \\ a_{21} & a_{22} & \cdots & \cdots & a_{2n} \\ \vdots & \vdots & \cdots & \cdots & \vdots \\ \vdots & \vdots & \cdots & \cdots & \vdots \\ a_{n1} & a_{n2} & \cdots & \cdots & a_{nn} \end{bmatrix} \tag{14}$$

where a_{ij} is equal to 1 and a_{ij} is equal to $1/a_{ji}$ In this study, the correlation of determinants of the variables is used to construct this matrix.

After that, the vector of weights, $w = w_1, w_2, w_3, \ldots, w_n$ is calculated based on Saaty's eigenvector [71].

The normalization method is applied to normalize the eigenvector using the following formula:

$$a_{ij} = \frac{a_{ij}}{\sum_{j=1}^{n} a_{ij}} \quad (15)$$

Thereafter, the weights are computed using the following formula:

$$w_1 = \frac{\sum_{j=1}^{n} a_{ij}}{n} \quad (16)$$

where $i, j = 1,2, 3, \ldots, n$.

A consistency ratio (CR) of the pairwise comparison in the AHP process has been determined by dividing the consistency index (CI) by the random index proposed in [70]. The following formula is mentioned:

$$CI = \frac{\lambda_{max} - n}{n - 1} \quad (17)$$

where CI is the consistency index, n is the number of elements being compared in the matrix, and λ_{max} is the largest or principal eigenvalue of the matrix. The consistency ratio (CR) is calculated using the following formula:

$$CR = \frac{CI}{RI} \quad (18)$$

where CR = consistency ratio (acceptable consistency ratio is $\leq$0.10 and inadequate consistency ratio is $\geq$0.10; [70]), CI = consistency index, and RI = random index.

In the present study, 1.54 is considered as a random index (RI) comprising 12 elements that have been measured and referenced in [73,74].

The composite flood vulnerability index (CFVI), based on [75], of the wards in the study area, is obtained in the final step by adding the ratings of each alternative to the weights of the sub-criteria to calculate the flood vulnerability index. Five categories—very high, high, moderate, low, and very low flood vulnerability—have been recognized for the CFVI of the selected study area.

3.4.4. Composite Ibrahim Index (CIb) of Socio-Economic Development

The Ibrahim index [76,77] has been used to standardize the data for calculating the socio-economic status of urban development.

Here,

$$Ibrahim\ Index(I_b) = \frac{X_t \sim Min\ (X)}{Max\ (X) - Min\ (X)} \times 100 \quad (19)$$

where X_t = the actual value of a particular indicator for the socio-economic status of urban development in the wards of Nabadwip Municipality in the year t, and *Min (X) and Max (X)* = the minimum and maximum values for the particular indicator of socio-economic status of urban development throughout the entire period of all the wards in Nabadwip Municipality area.

The composite Ibrahim index (CI_b) has been calculated to measure the level of the socio-economic status of urban development in the wards of Nabadwip Municipality in 2015. For calculating the composite Ibrahim index, the following formula has been used:

$$CI_b = \frac{(I_bA + I_bB + I_bTC + \ldots + I_bV)}{23} R \quad (20)$$

where CI_b = composite Ibrahim index and I_b= Ibrahim index.

The selected indicators [19] are as follows:

I_bA is the total household/1;000;000 population;

I_bB is the total Scheduled Caste (SC) population/1000 population;

I_bC is the total Scheduled Tribe (ST) population/1000 population;
I_bD is the total literates/1000 population;
I_bE is the total workers/1000 population;
I_bF is the number of secondary and higher secondary schools/1000 population;
I_bG is the number of nursing homes/1000 population;
I_bH is the road length/square km (1 square km = 0.386102 square mile);
I_bI is the dumping sites/square km;
I_bK is the pumping stations/square km;
I_bJ is the water-holding capacity of pumping stations/square km;
I_bL is the number of waterbodies/square km;
I_bM is the height of waterlogging/square km;
I_bN is the number of banks/square km;
I_bO is the number of ATMs/square km
I_bP is the number of temples/square km;
I_bQ is the number of hotels/square km;
I_bR is the distance of the center of the municipal ward from the station;
I_bS is the distance of the center of the municipal ward from the bus stand;
I_bT is the distance of the center of the municipal ward from the Municipality Office;
I_bU is the distance of the center of the municipal ward from the Police Station;
I_bV is the distance of the center of the municipal ward from the Post Office;
I_bW is the distance of the center of the municipal ward from the State General Hospital.

Based on the calculated composite Ibrahim index, the wards of Nabadwip Municipality have been categorized into five zones of the composite Ibrahim index: notably high, moderately high, moderately low, and low socio-economic status of urban development.

3.4.5. Correlation, Regression, Hypothesis Testing, and Model Validation

A multiple linear regression model has been used in the present study to predict the NDFI based on the selected flood vulnerability factors. To clarify the nature of autocorrelation among independent variables and the validity of the model, autocorrelation values are also extracted in the regression model. In addition to the coefficients of determinants, significance tests and analysis of variance (ANOVA) have been adopted in the analysis of the multiple linear regression model.

The formula of the multiple linear regression model [78] is based on [79,80] and is

$$Y = \beta_0 + \beta_1 X_1 + \ldots + \beta_n X_n + e_t \quad (21)$$

where Y is the dependent variable (here, normalized difference flood index (NDFI)), X_1 is the independent variable, β_1 is a parameter, and e_t is the error.

Here, the correlation coefficient (r) and coefficient of determinants (r^2) values are calculated using Pearson's formula.

The formula of 'R' (multiple correlation coefficient) [79,80] is

$$R = \sqrt{\frac{\left[\left(r.yx_1\right)^2 + \left(r.yx_2\right)^2\right] - \left(2 \times r.yx_1 \times r.yx_2 \times r.x_1 \times 2\right)}{1 - \left(r.x_1x_2\right)^2}d} \quad (22)$$

where R is the value of the correlation coefficient, x_1 is one independent variable, x_2 is another independent variable, and y is the dependent variable.

Autocorrelation has been determined using the 'Durbin–Watson test' [81] with 99% and 95% confidence intervals [82]. The formula of the Durbin–Watson test adopted by [83] is

$$d = \frac{\sum_{t=2}^{n}\left(t - t-1\right)^2}{\sum_{t=1}^{n}\left(t\right)^2}F \quad (23)$$

where d = Durbin and Watson statistic (DW statistic) and e_t = error term.

To identify the *f*-statistics, ANOVA has been run using the following formula.
The '*F*' value in the 'j^{th}'one-way ANOVA' [84] is calculated using the following formula:

$$F = \frac{Explained\ variance}{Unexplained\ variance} \tag{24}$$

$$\text{or, } F = \frac{Between - group\ variability}{Within - group\ variability} \tag{25}$$

The 'explained variance' or 'between-group variability' is

$$\sum_{i=1}^{k} ni(\bar{Y}i. - \bar{Y})2/(K-1) \tag{26}$$

where $\bar{Y}i$ denotes the sample mean in the i^{th} group, ni is the number of observations in the i^{th} group, $\bar{Y}$ denotes the overall mean of the data, and *K* denotes the number of groups.

The 'unexplained variance' or 'within-group variability' is

$$\sum_{i=1}^{n} . \sum_{j=1}^{ni} (Yij - \bar{Y}i.)2/(N-K) \tag{27}$$

where *Yij* is the observation in the i^{th} out of *K* groups and *N* is the overall sample size.

This *F*-statistic follows the *F*-distribution with *K-1*, *N-K* degree of freedom (df) under the null hypothesis.

A two-sample *t*-test with unequal variance has been used to test the hypotheses. Here, the hypothesis has been tested using data from two statistical populations (variable 1: CFVI; variable 2: CIb). The formula of 'Welch's t test' [85] is

$$t = \frac{x_1 - x_2}{\sqrt{\frac{s_1^2}{n_1} + \frac{s_2^2}{n_2}}} \tag{28}$$

where *t* is the *t*-statistic.

In the present study, x_1 *and* x_2 are the population means, s_1 and s_2 are the population variances. and n_1 and n_2 are the total number of statistical population 1 and statistical population 2.

During hypothesis testing, it can be theorized that

Null hypothesis (H_0). *μ1 = μ2 (when the null hypothesis indicates that the means of the two statistical populations are equal).*

Alternative hypothesis (H_1). *μ2 ≠ μ1 (when the alternative hypothesis indicates that the means of the two statistical populations are unequal). In this study, the statistical software calculated Welch's degrees of freedom and used a 95% confidence interval.*

For the years 2000 and 2015 in the study area, a receiver operating characteristic (ROC) curve and area under the ROC curve (AUC) have been constructed to validate the flood vulnerability index model. The probability is graphically plotted using the ROC curve, and additionally, the true positive rate of 1-sensitivity and the false positive rate of specificity are used to calculate the area under the ROC curve (AUC) [86,87]. The overall efficiency of flood susceptibility was evaluated using ROC-AUC in an earlier study on Iran [88]. The research was also conducted [89] to assess the precision of the mapping of flood risk using ROC-AUC. ROC-AUC was used to validate the mapping of flood risk zones in Prayagraj, India [90].

4. Results

4.1. An Outline of Rainfall Situation and Flood Occurrences in Nabadwip Municipality

Nabadwip Municipality faced major flood situations from 2000 to 2020. It is noteworthy that they occurred in the years 2000, 2006, 2007, and 2015. The most effective floods, concerning the overall situation, were in 2000 and 2015. In 2000, the average monthly rainfall was 118.96 millimeters (mm), and in 2015, it was 113.01 mm, where the annual rainfall was 1427.57 mm and 1356.13 mm, respectively (Figure 3). The peak season of monthly rainfall in 2000 and 2015 occurred in July, August, September, and October (Figures 4–7). The report [91] states that in 2000, a flood incident occurred on September 17 and lasted through the second week of October due to heavy rainfall and discharge flow. A flooding incident occurred in 2015 starting on July 24 due to a strong cyclonic storm and associated heavy rainfall [92]. The daily rainfall situation (Figures 4–7) showed the strongest uptrend pattern on 6 June, 22 July, 29 August, and 19 September in 2000 and on 27 June, 28 July, 1 August, and 21 September in 2015. The SPI values show the standardized deviation of monthly rainfall over 30 years (1986–2015; Table 4); in addition, SPI values of the study area for 1 month, 3 months, 4 months, 6 months, and 12 months in the years 2000 and 2015 are shown (Table 5). Figures 8–12 show 1-month SPI, 3-month SPI, 4-month SPI, 6-month SPI, and 12-month SPI, respectively, from 2000 to 2015 (a total of 16 years). In 2000, the SPIs from June to September were 0.75, 0.55, −0.26, and 0.04; in 2015, the values were −0.81, −0.74, 1.24, and −0.47, respectively. That indicates a higher consistency of rainfall in 2000 than in 2015. The Nabadwip Municipality area experiences humid weather conditions, as indicated by the highest positive SPI value from August to September 2015. The flood in Nabadwip in 2000 had the highest water level ever recorded during a flood situation. In wards 6, 7, 8, 10, 14, 15, 21, and 22, the water levels reached a depth of more than 10 feet (3.048 m) (Figure 13).

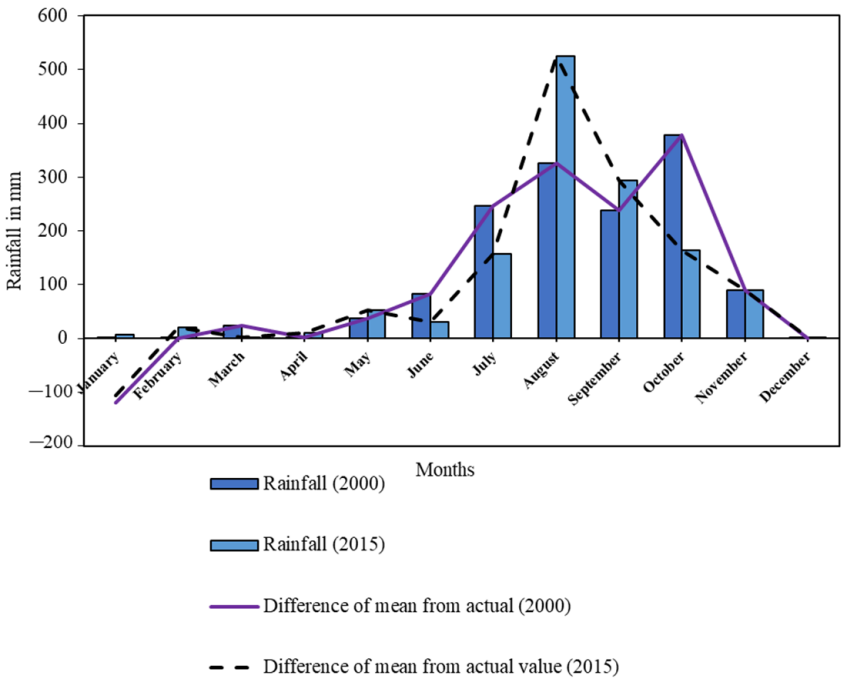

Figure 3. Annual rainfall situation of 2000 and 2015.

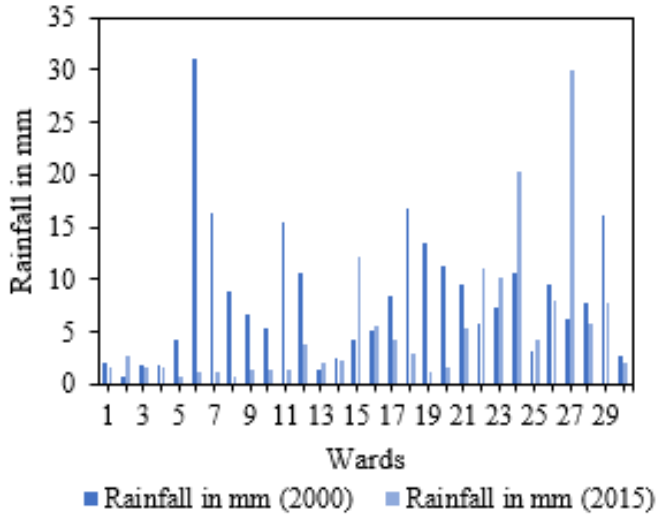

Figure 4. Daily rainfall situation (June 2000 and 2015).

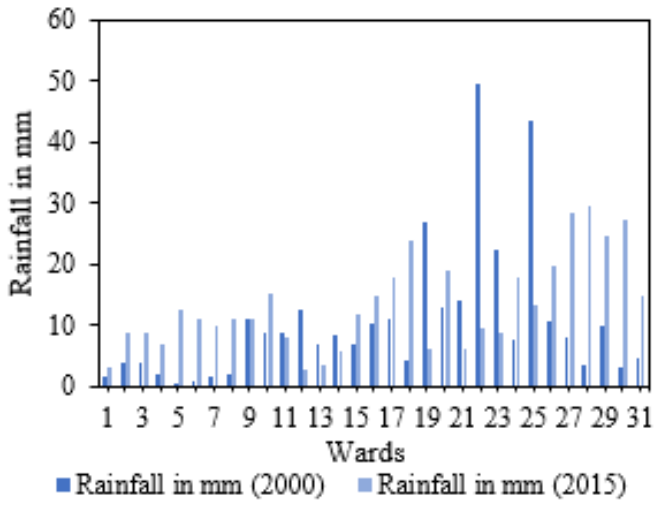

Figure 5. Daily rainfall situation (July 2000 and 2015).

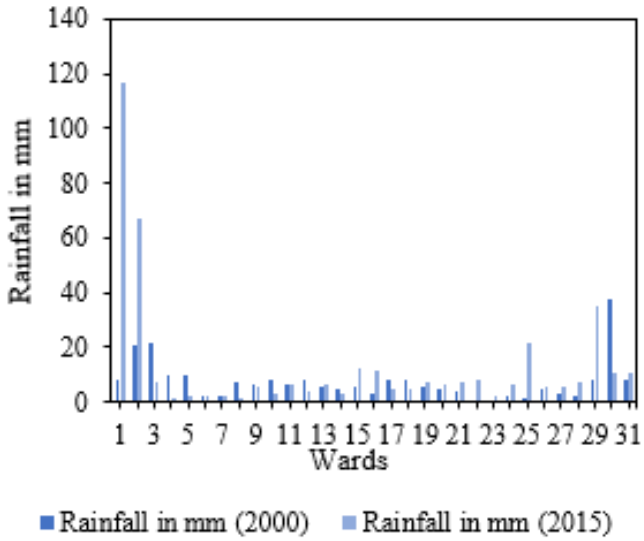

Figure 6. Daily rainfall situation (August 2000 and 2015).

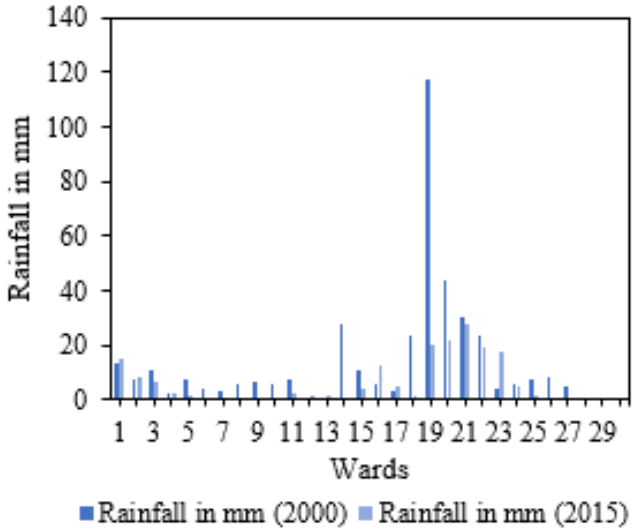

Figure 7. Daily rainfall situation (September 2000 and 2015).

Table 4. Monthly SPI values of average rainfall condition in Nabadwip Municipality area (1986–2015).

Year	Month	SPI	Year	Month	SPI	Year	Month	SPI
1986	1	−0.48	1996	1	−0.70	2006	1	0.33
1986	2	0.43	1996	2	0.05	2006	2	−1.84
1986	3	0.37	1996	3	−0.07	2006	3	−0.65
1986	4	−0.58	1996	4	−0.15	2006	4	0.00
1986	5	−0.33	1996	5	0.21	2006	5	0.07
1986	6	−0.94	1996	6	−1.12	2006	6	1.01
1986	7	0.57	1996	7	0.07	2006	7	0.86
1986	8	−0.74	1996	8	−0.57	2006	8	1.34
1986	9	−2.29	1996	9	1.63	2006	9	0.35
1986	10	0.44	1996	10	−1.46	2006	10	0.37
1986	11	0.63	1996	11	−0.10	2006	11	−0.54
1986	12	1.53	1996	12	−0.96	2006	12	0.29
1987	1	1.05	1997	1	−0.53	2007	1	−0.44
1987	2	0.45	1997	2	1.47	2007	2	−1.57
1987	3	−0.61	1997	3	0.13	2007	3	2.08
1987	4	−0.33	1997	4	0.77	2007	4	−0.23
1987	5	0.43	1997	5	0.95	2007	5	0.16
1987	6	−0.93	1997	6	−0.78	2007	6	−0.32
1987	7	−2.45	1997	7	−0.07	2007	7	−0.55
1987	8	−1.18	1997	8	1.90	2007	8	2.29
1987	9	−1.19	1997	9	1.10	2007	9	−0.25
1987	10	−0.98	1997	10	−0.91	2007	10	1.27
1987	11	−1.78	1997	11	−2.52	2007	11	0.15
1987	12	0.39	1997	12	0.06	2007	12	1.04
1988	1	1.05	1998	1	1.82	2008	1	−0.35
1988	2	−1.58	1998	2	1.54	2008	2	1.99

Table 4. *Cont.*

Year	Month	SPI	Year	Month	SPI	Year	Month	SPI
1988	3	1.22	1998	3	0.11	2008	3	1.04
1988	4	−0.02	1998	4	2.25	2008	4	−0.24
1988	5	−0.39	1998	5	−0.17	2008	5	−0.65
1988	6	−0.09	1998	6	−0.13	2008	6	−0.07
1988	7	1.10	1998	7	1.47	2008	7	0.56
1988	8	−1.37	1998	8	0.66	2008	8	0.44
1988	9	−0.89	1998	9	0.76	2008	9	−0.14
1988	10	−0.59	1998	10	0.49	2008	10	0.48
1988	11	−1.40	1998	11	0.70	2008	11	0.77
1988	12	1.18	1998	12	0.92	2008	12	−0.68
1989	1	0.06	1999	1	−0.32	2009	1	−0.22
1989	2	−1.16	1999	2	−1.70	2009	2	−0.85
1989	3	−0.30	1999	3	−0.96	2009	3	−0.79
1989	4	0.07	1999	4	−0.42	2009	4	−0.11
1989	5	−0.63	1999	5	−1.64	2009	5	−0.88
1989	6	1.12	1999	6	0.94	2009	6	1.00
1989	7	−0.20	1999	7	−0.26	2009	7	−1.64
1989	8	−0.31	1999	8	1.44	2009	8	−0.41
1989	9	−1.26	1999	9	1.12	2009	9	0.45
1989	10	−0.11	1999	10	1.53	2009	10	0.18
1989	11	0.95	1999	11	0.83	2009	11	−0.01
1989	12	−1.24	1999	12	0.00	2009	12	0.74
1990	1	0.88	2000	1	−0.27	2010	1	−0.36
1990	2	−0.58	2000	2	−0.61	2010	2	−0.92
1990	3	0.81	2000	3	0.97	2010	3	−0.20
1990	4	1.61	2000	4	−0.24	2010	4	−0.22
1990	5	0.99	2000	5	0.93	2010	5	−0.29
1990	6	2.23	2000	6	0.55	2010	6	0.67
1990	7	−0.27	2000	7	−0.01	2010	7	−0.62
1990	8	0.28	2000	8	−0.13	2010	8	−0.88
1990	9	−0.86	2000	9	−0.79	2010	9	−2.06
1990	10	−0.54	2000	10	0.49	2010	10	−0.27
1990	11	1.02	2000	11	−0.48	2010	11	0.46
1990	12	1.30	2000	12	−0.68	2010	12	−0.10
1991	1	0.45	2001	1	−1.47	2011	1	1.28
1991	2	1.17	2001	2	0.18	2011	2	−0.70
1991	3	−0.67	2001	3	−0.16	2011	3	0.02
1991	4	−0.13	2001	4	1.51	2011	4	0.48
1991	5	−1.11	2001	5	−0.50	2011	5	0.36
1991	6	−0.76	2001	6	0.25	2011	6	0.08
1991	7	0.05	2001	7	1.45	2011	7	0.73

Table 4. *Cont.*

Year	Month	SPI	Year	Month	SPI	Year	Month	SPI
1991	8	−0.77	2001	8	0.34	2011	8	−0.71
1991	9	0.45	2001	9	0.36	2011	9	0.95
1991	10	0.16	2001	10	−0.75	2011	10	0.02
1991	11	0.77	2001	11	1.28	2011	11	−1.55
1991	12	0.30	2001	12	0.67	2011	12	−0.52
1992	1	1.66	2002	1	−0.41	2012	1	−0.26
1992	2	−0.25	2002	2	1.09	2012	2	1.31
1992	3	0.39	2002	3	−1.21	2012	3	−0.09
1992	4	−0.22	2002	4	0.07	2012	4	−0.66
1992	5	−0.52	2002	5	−0.42	2012	5	0.44
1992	6	−0.42	2002	6	0.07	2012	6	−0.83
1992	7	−1.07	2002	7	0.22	2012	7	−1.58
1992	8	−0.03	2002	8	0.46	2012	8	−0.98
1992	9	−0.38	2002	9	1.09	2012	9	−0.52
1992	10	−1.07	2002	10	0.50	2012	10	0.95
1992	11	−1.02	2002	11	−0.29	2012	11	−0.27
1992	12	−0.25	2002	12	1.29	2012	12	0.25
1993	1	−0.45	2003	1	−0.56	2013	1	1.20
1993	2	−0.32	2003	2	−0.10	2013	2	0.16
1993	3	−0.14	2003	3	−0.14	2013	3	0.29
1993	4	0.67	2003	4	1.28	2013	4	−0.84
1993	5	1.60	2003	5	1.38	2013	5	0.04
1993	6	−0.37	2003	6	−0.33	2013	6	1.78
1993	7	1.16	2003	7	1.29	2013	7	0.96
1993	8	−0.33	2003	8	0.39	2013	8	−0.98
1993	9	1.07	2003	9	−0.44	2013	9	0.84
1993	10	0.66	2003	10	−0.59	2013	10	1.17
1993	11	−0.45	2003	11	1.25	2013	11	0.96
1993	12	0.63	2003	12	−0.20	2013	12	−0.71
1994	1	−0.88	2004	1	1.65	2014	1	−0.33
1994	2	0.68	2004	2	−0.02	2014	2	0.03
1994	3	1.81	2004	3	0.34	2014	3	1.62
1994	4	0.12	2004	4	−0.08	2014	4	0.16
1994	5	0.83	2004	5	1.16	2014	5	−1.78
1994	6	−0.65	2004	6	−0.52	2014	6	0.09
1994	7	1.03	2004	7	0.41	2014	7	−0.91
1994	8	−0.27	2004	8	0.70	2014	8	−0.96
1994	9	0.31	2004	9	0.30	2014	9	0.66
1994	10	−0.89	2004	10	2.53	2014	10	−1.20
1994	11	−0.56	2004	11	0.97	2014	11	−0.97
1994	12	−0.65	2004	12	−0.65	2014	12	−1.53

Table 4. *Cont.*

Year	Month	SPI	Year	Month	SPI	Year	Month	SPI
1995	1	0.00	2005	1	−0.17	2015	1	0.59
1995	2	−0.11	2005	2	0.65	2015	2	1.15
1995	3	0.26	2005	3	−0.46	2015	3	−0.27
1995	4	−0.45	2005	4	1.49	2015	4	0.37
1995	5	−1.79	2005	5	1.71	2015	5	1.45
1995	6	1.76	2005	6	−0.30	2015	6	−0.48
1995	7	1.02	2005	7	−0.91	2015	7	−0.80
1995	8	0.51	2005	8	−0.06	2015	8	1.42
1995	9	1.42	2005	9	0.36	2015	9	−0.29
1995	10	1.08	2005	10	−0.26	2015	10	−1.02
1995	11	0.20	2005	11	2.14	2015	11	−0.46
1995	12	2.16	2005	12	−0.43	2015	12	−0.33

Source: Calculated by the authors.

Table 5. Monthly standardized precipitation index (SPI) of the years 2000 and 2015.

Months	Jan	Feb	Mar	Apr	May	Jun	Jul	Aug	Sep	Oct	Nov	Dec
SPI 1-month												
2000	1	0.05	−0.46	0.94	−0.29	0.75	0.55	0.04	−0.26	−1.17	−0.64	−0.49
2015	0.82	1.11	−0.11	0.38	1.29	−0.81	−0.74	1.24	−0.47	−1.22	−0.63	−0.11
SPI 3-month												
2000	NA	NA	0.17	−0.02	0.51	0.49	0.20	−0.14	−0.72	−0.45	−0.70	−0.27
2015	−1.29	0.29	0.34	0.21	0.53	−0.15	−0.73	0.16	0.07	−0.28	−1.51	−1.52
SPI 4-month												
2000	NA	NA	NA	−0.42	0.25	0.73	0.13	−0.08	−0.61	−0.40	−0.74	−0.73
2015	−2.20	−1.13	−0.09	0.12	0.78	−0.54	−0.71	0.28	−0.09	−0.57	−0.59	−1.52
SPI 6-month												
2000	NA	NA	NA	NA	NA	0.41	0.13	−0.08	−0.59	−0.30	−0.58	−0.67
2015	−1.49	−1.30	−2.14	−1.35	0.42	−0.32	−0.76	0.21	0.01	−0.59	−0.90	−0.82
SPI 12-month												
2000	NA	NA	NA	NA	NA	NA	NA	NA	NA	NA	NA	−0.60
2015	−1.61	−1.53	−1.65	−1.64	−1.50	−1.68	−1.73	−0.88	−1.23	−0.91	−0.85	−0.81

NA: Not applicable. **Source:** Calculated by the authors.

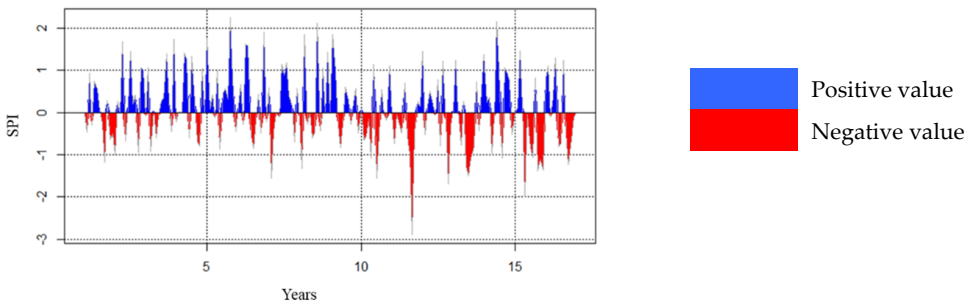

Figure 8. One-month SPI (years: 2000–2015).

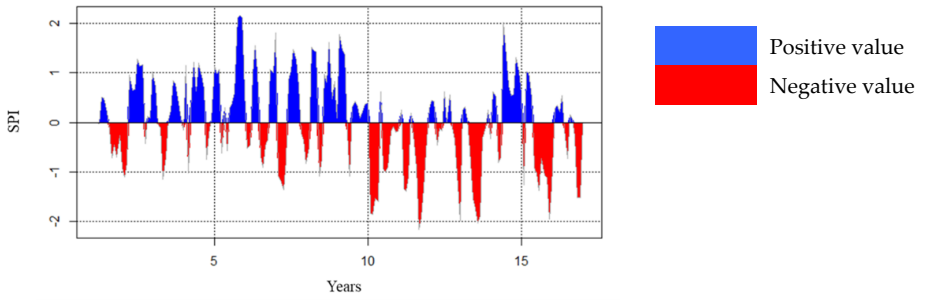

Figure 9. Three-month SPI (years: 2000–2015).

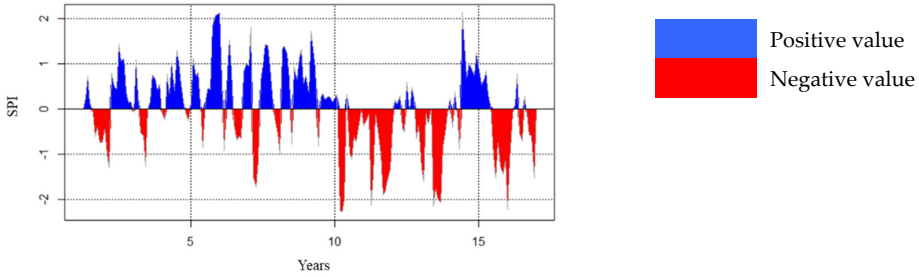

Figure 10. Four-month SPI (years: 2000–2015).

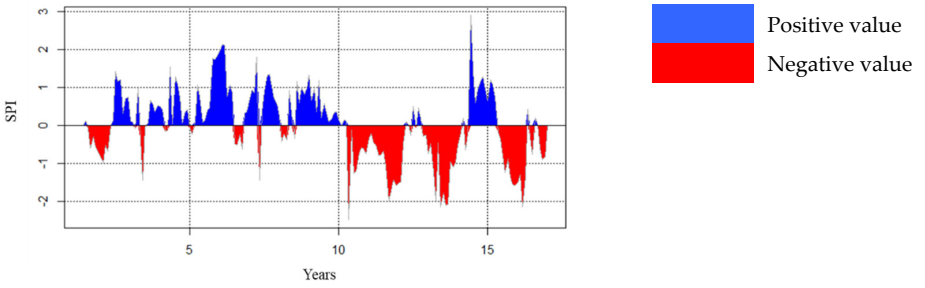

Figure 11. Six-month SPI (years: 2000–2015).

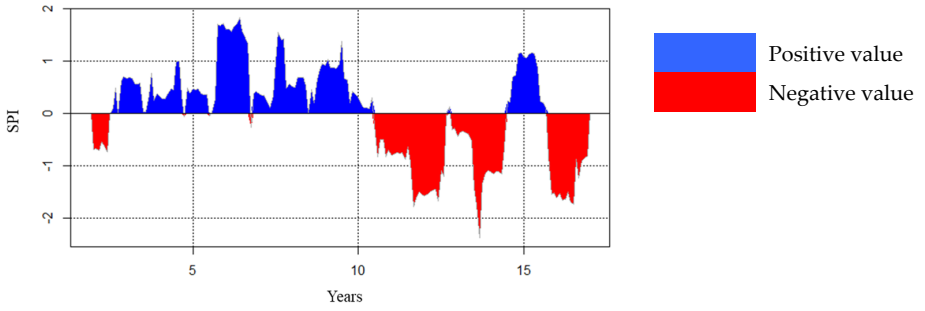

Figure 12. Twelve-month SPI (years: 2000–2015).

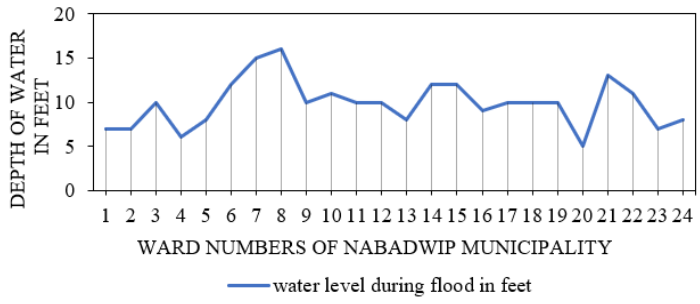

Figure 13. The water level during the recent flood in Nabadwip.

4.2. Factors and Zonation of Flood Vulnerability

The following physical factors have been specifically related to flood vulnerability: relief (DEM), slope, flow direction, flow distance, flow length density (stream density), NDVI, NDWI (and MNDWI), NDBI, NDSI, NDTI, and the distance between municipal wards and the old and new river courses (Figures 14–42). The present study examines the relationships between the variables (Tables 6 and 7) concerning their situations in 2000 and 2015. Significant positive or negative correlations between NDVI and NDTI, NDWI and NDBI, NDSI and NDTI, NDBI with NDSI and NDTI, and between the distance of municipal wards from the old river course and the distance between municipal wards have been found. The correlation values are greater than 0.7. Significant positive or negative correlations between NDVI and NDTI, NDWI and NDBI, NDBI, and NDTI, and between the distance of municipal wards from the old river course and the distance of municipal wards from the new river course have been depicted in 2015. The spatial distribution of the normalized difference flood index (NDFI) in 2000 and 2015 is depicted in Figures 28 and 43, respectively. The majority of the areas in Nabadwip Municipality had moderate NDFI values between 2000 and 2015. A low value (−0.131) of NDFI2 was found in the northwestern, northeastern, eastern, southern, and southeastern portions of the municipality area in a dispersed condition in 2000, whereas a high value (0.952) of NDFI2 had been found in the northernmost, southernmost, western, and southeastern portions of the municipality area. The NDFI2 condition in 2015 was quite similar to that of 2000, but the range of the index was higher (the high value was 0.866 and the low value was −0.301). To determine the prediction value of the normalized difference flood index 2 (NDFI2) in 2015 by each predictor of flood vulnerability, a multiple linear regression model has been formulated. The relationships among the predictors have been represented in Tables 6 and 7. Table 8 displays the mean and standard deviation of the selected dependent variable along with the independent variables for 2015. Elevation (relief) shows the highest standard deviation (SD) (mean = 16.15, SD = 2.64), and flow distance shows the lowest (mean = 1.88, SD = 2.02). The NDFI2 and its predictors had a very strong relationship, as evidenced by the correlation coefficient of 0.866 (Table 9). In this instance, a significant change of 1 unit in each predictor indicates a change of 75% in NDFI2 (F 0.05) (Tables 9 and 10). Due to the presence of autocorrelation (DW = 2.513), the coefficient values for NDVI and NDBI are not considered (Tables 9 and 11). In 2015, NDFI2, the dependent variable, was predicted by the other variables either significantly or insignificantly (Table 11). Here, NDFI2 increased with increasing ground elevation, slope, flow direction, flow length line density, NDWI, and NDTI, and decreased with decreasing flow distance, NDSI, the distance of municipal wards from the old river course, and the distance of municipal wards from the new river course. The highly influential factors were flow length and line density, NDWI, NDSI, NDTI, the distance of municipal wards from the old river course, and the distance of municipal wards from the new river course in 2015. Here, a 1 km/square km (0.621371 mile/0.38610191964 square mile) increase in flow length line density resulted in a 5.4% increase in NDFI2, a 1-unit increase in NDWI resulted in a 4.599-unit increase in NDFI2, a 1-unit increase in NDSI resulted in a 5.790-unit decrease in NDFI2, a 1-unit increase in NDTI resulted in a 6.476-unit increase in NDFI2, and a 1 km (0.621371 miles) increase in the distance of municipal wards from the old river course resulted in a 10.6% decrease in NDFI2.

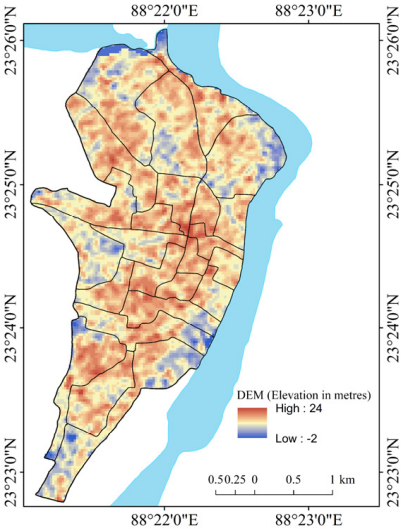

Figure 14. Relief (2000).

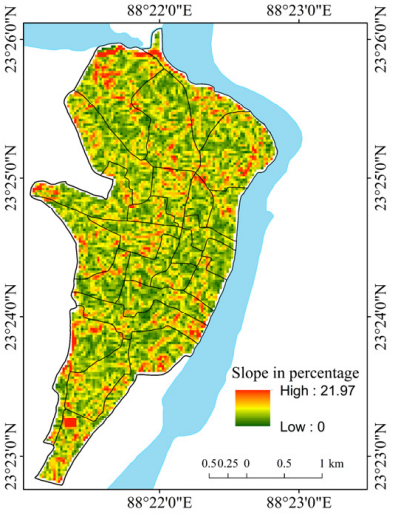

Figure 15. Slope (2000).

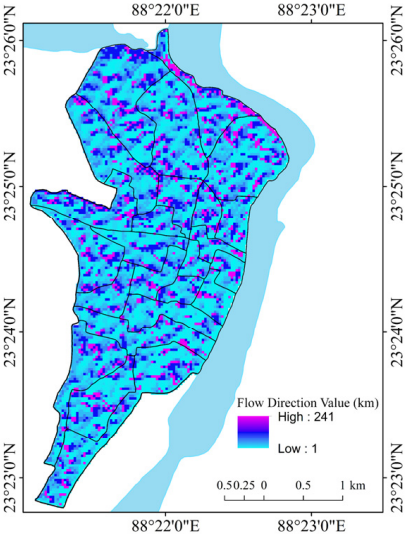

Figure 16. Flow direction (2000).

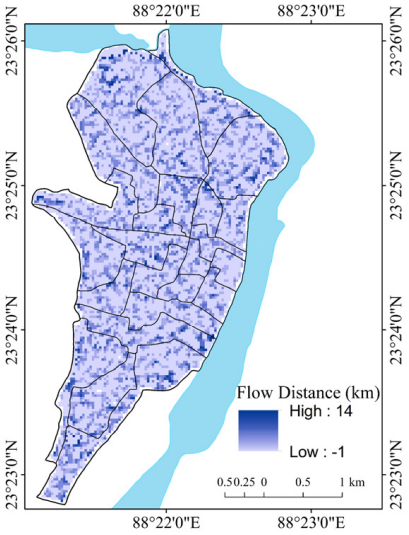

Figure 17. Flow distance (2000).

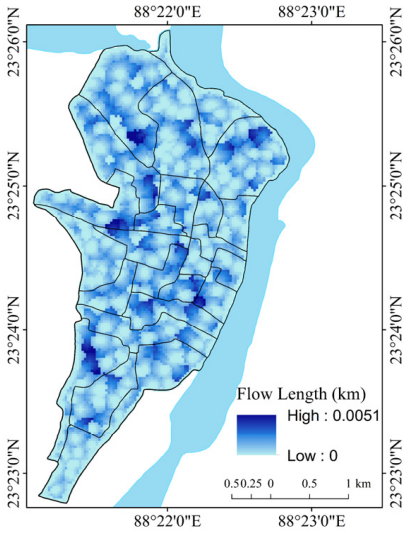

Figure 18. Flow length (2000).

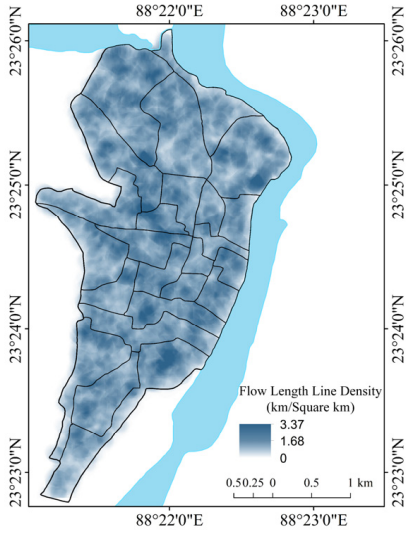

Figure 19. Flow length line density (2000).

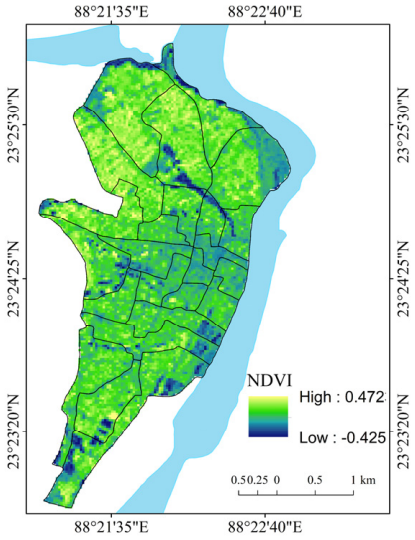

Figure 20. NDVI (2000).

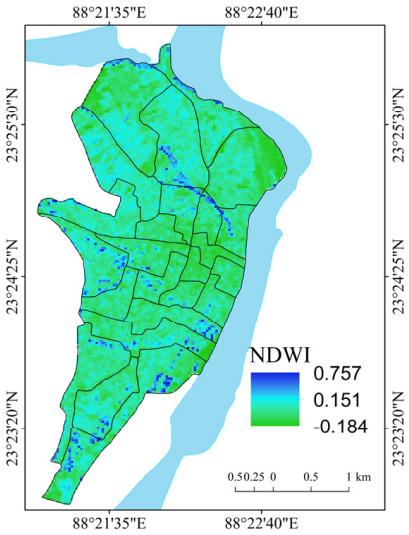

Figure 21. NDWI (2000).

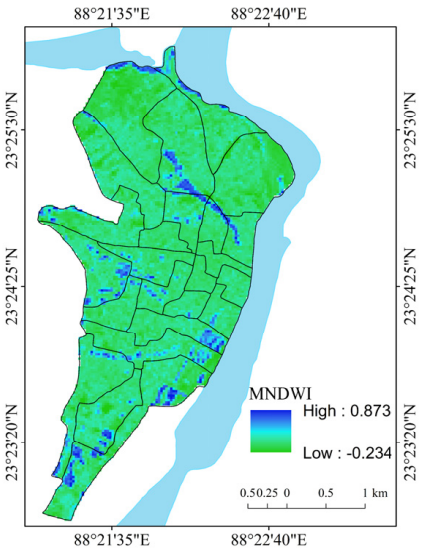

Figure 22. MNDWI (2000).

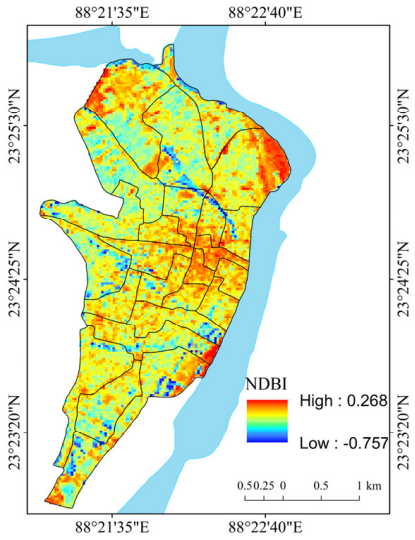

Figure 23. NDBI (2000).

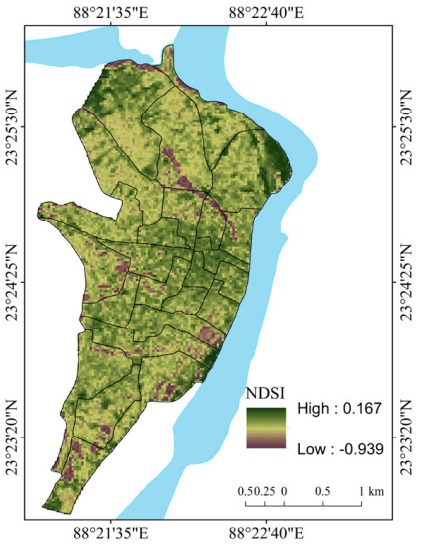

Figure 24. NDSI (2000).

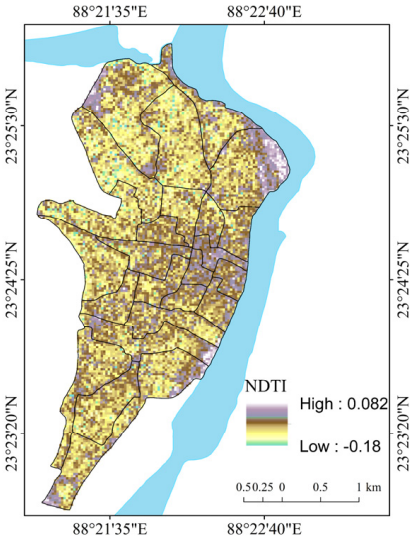

Figure 25. NDTI (2000).

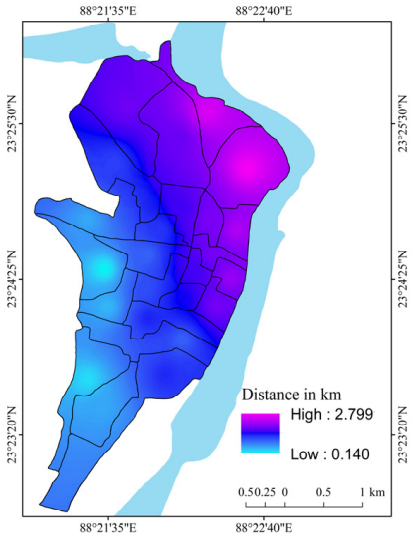

Figure 26. Distance of the centers of the municipal wards from the old river course (2000).

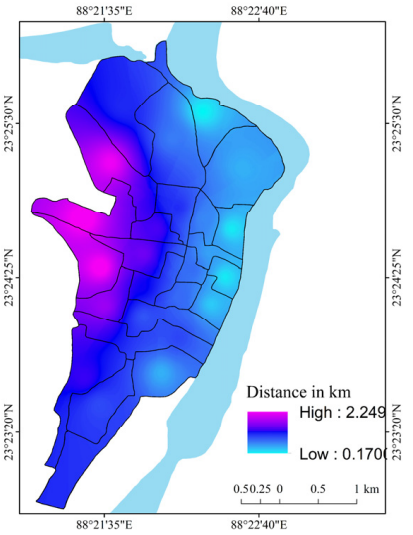

Figure 27. Distance of the centers of the municipal wards from the new river course (2000).

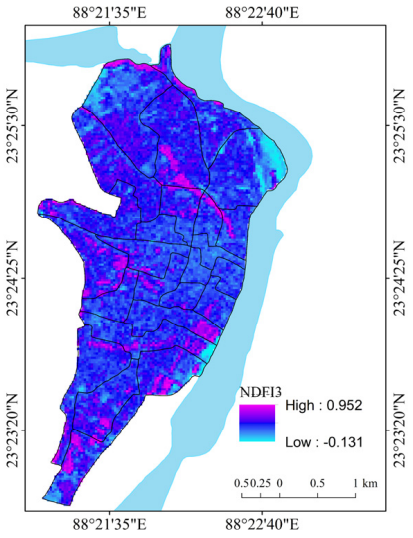

Figure 28. NDFI2 (2000).

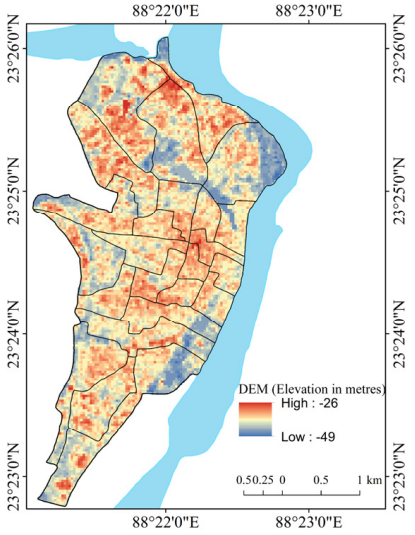

Figure 29. Relief (2015).

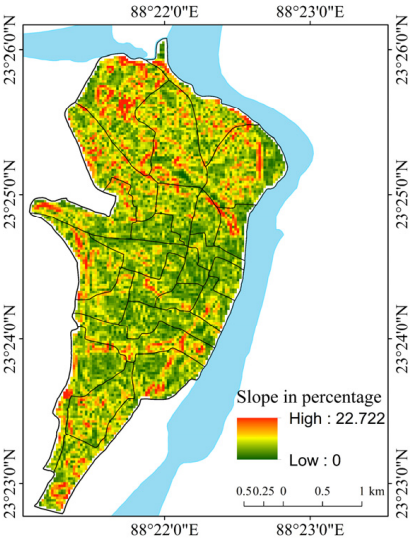

Figure 30. Slope (2015).

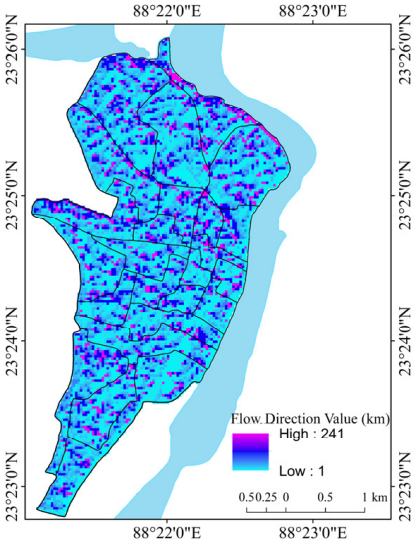

Figure 31. Flow direction (2015).

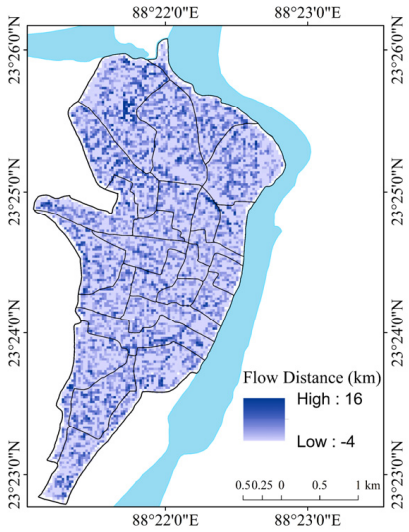

Figure 32. Flow distance (2015).

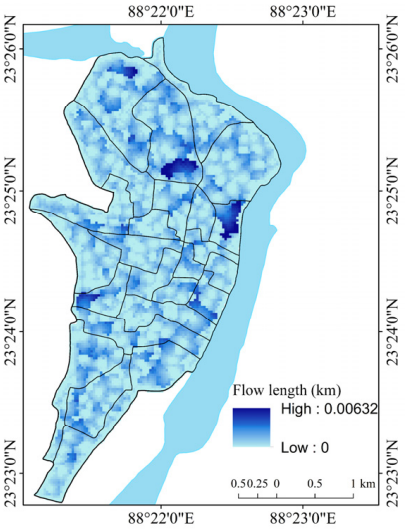

Figure 33. Flow length (2015).

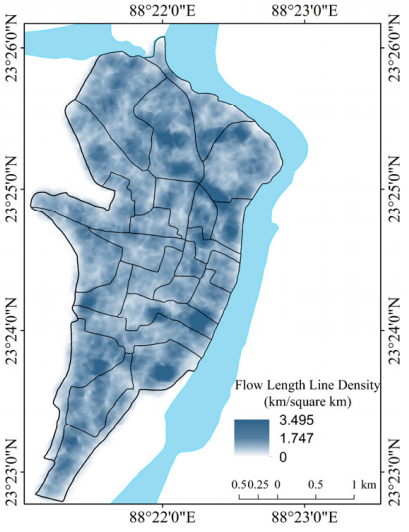

Figure 34. Flow length line density (2015).

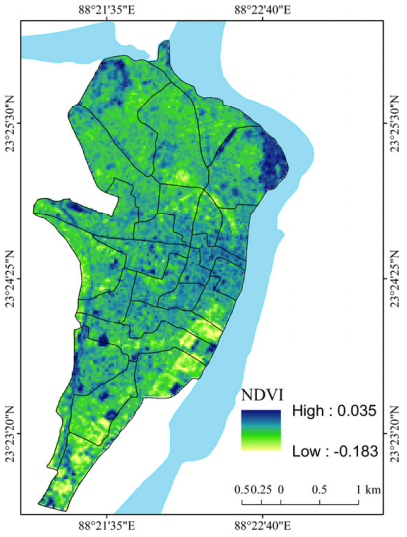

Figure 35. NDVI (2015).

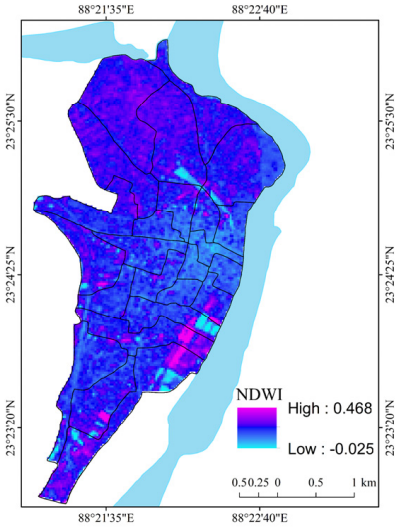

Figure 36. NDWI (2015).

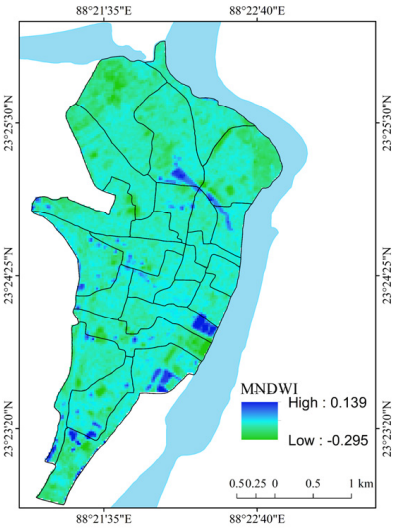

Figure 37. MNDWI (2015).

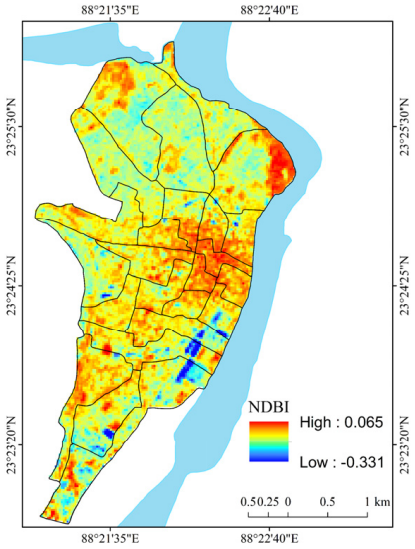

Figure 38. NDBI (2015).

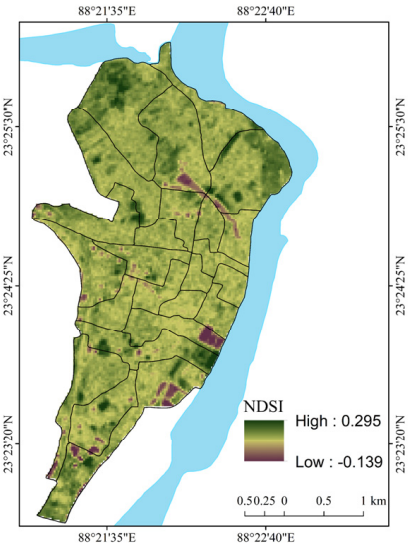

Figure 39. NDSI (2015).

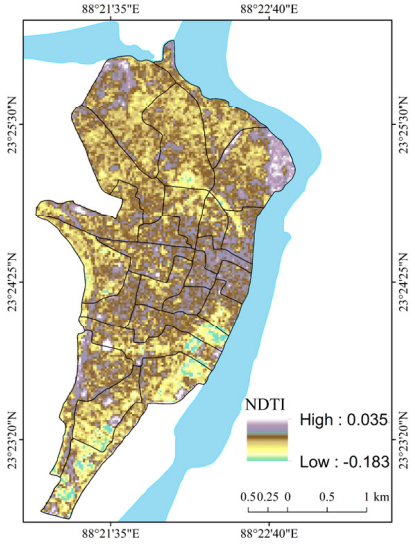

Figure 40. NDTI (2015).

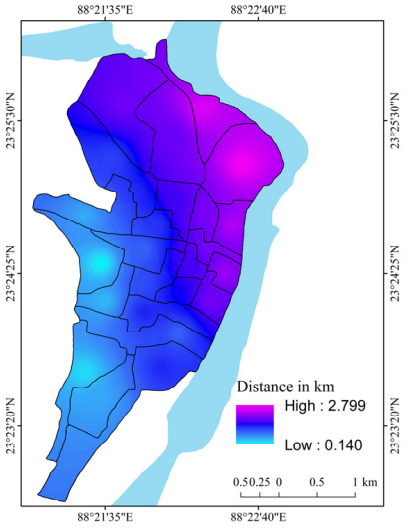

Figure 41. Distance of the centers of the municipal wards from the old river course (2015).

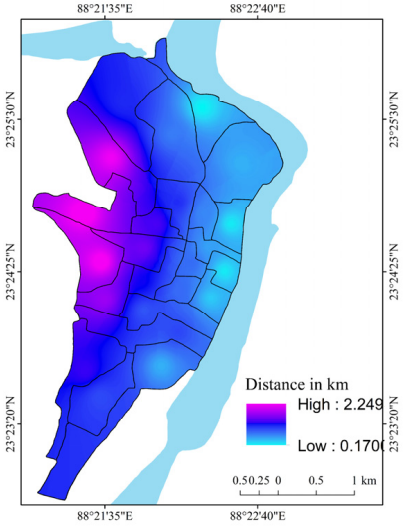

Figure 42. Distance of the centers of the municipal wards from the new river course (2015).

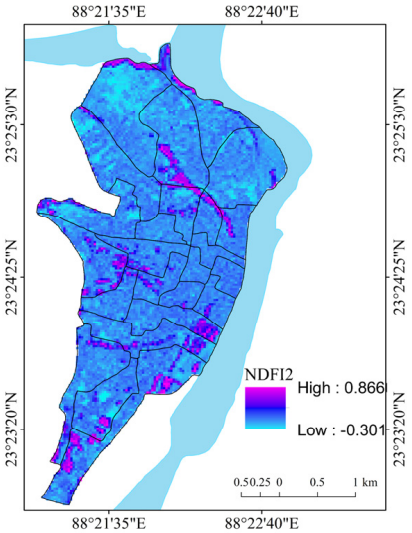

Figure 43. NDFI2 (2015).

Table 6. Correlation matrix of the selected indicators of flood vulnerability (2000).

	R-Value											
	Elevation	**Slope**	**Flow Direction**	**Flow Distance**	**Flow Length Line Density**	**NDVI**	**NDWI**	**NDBI**	**NDSI**	**NDTI**	**Distance of Municipal Wards from the Old River Course**	**Distance of Municipal Wards from the New River Course**
Elevation	1.000	−0.086	0.062	0.368	−0.277	−0.118	0.024	−0.024	−0.066	−0.150	−0.168	0.117
Slope	−0.086	1.000	−0.080	0.443 *	0.018	0.058	−0.092	0.092	0.015	0.017	0.502 *	−0.397
Flow Direction	0.062	−0.080	1.000	−0.288	−0.143	−0.089	−0.053	0.053	−0.067	0.040	−0.137	0.244
Flow Distance	0.368	0.443 *	−0.288	1.000	−0.213	0.001	−0.070	0.070	0.047	0.081	0.058	−0.296
Flow Length Line Density	−0.277	0.018	−0.143	−0.213	1.000	−0.092	0.031	−0.031	−0.071	0.082	0.135	−0.291
NDVI	−0.118	0.058	−0.089	0.001	−0.092	1.000	0.676 **	−0.676	−0.464*	−0.771 **	−0.252	0.386
NDWI	0.024	−0.092	−0.053	−0.070	0.031	0.676 **	1.000	−1.000	−0.901 **	−0.718 **	−0.338	0.290
NDBI	−0.024	0.092	0.053	0.070	−0.031	−0.676 **	−1.000 **	1.000	0.901 **	0.718 **	0.338	−0.290
NDSI	−0.066	0.015	−0.067	0.047	−0.071	−0.464*	−0.901 **	0.901 **	1.000	0.690 **	0.246	−0.134
NDTI	−0.150	0.017	0.040	0.081	0.082	−0.771 **	−0.718 **	0.718 **	0.690 **	1.000	0.234	−0.327
Distance of municipal wards from the old river course	−0.168	0.502*	−0.137	0.058	0.135	−0.252	−0.338	0.338	0.246	0.234	1.000	−0.782 **
Distance of municipal wards from the new river course	0.117	−0.397	0.244	−0.296	−0.291	0.386	0.290	−0.290	−0.134	−0.327	−0.782 **	1.000

* Correlation is significant at the 0.05 level (2-tailed). <+ −0.3 0.3 to 0.7 >+ −0.7 . ** Correlation is significant at the 0.01 level (2-tailed). **Source:** Calculated by the authors.

Table 7. Correlation matrix of the selected indicators of flood vulnerability (2015).

	R-value											
	Elevation	**Slope**	**Flow Direction**	**Flow Distance**	**Flow Length Line Density**	**NDVI**	**NDWI**	**NDBI**	**NDSI**	**NDTI**	**Distance of Municipal Wards from the Old River Course**	**Distance of Municipal Wards from the New River Course**
Elevation	1.000	−0.634 **	−0.245	−0.259	−0.304	0.445 *	0.040	0.406 *	0.577 **	0.445 *	−0.168	0.117
Slope	−0.634 **	1.000	0.405*	0.604 **	0.378	−0.465 *	0.006	−0.380	−0.466 *	−0.465 *	0.188	−0.029
Flow Direction	−0.245	0.405 *	1.000	0.101	−0.058	−0.099	0.224	−0.185	0.132	−0.099	−0.106	0.234
Flow Distance	−0.259	0.604 **	0.101	1.000	−0.024	−0.318	0.272	−0.440 *	−0.106	−0.318	0.165	−0.083
Flow Length Line Density	−0.304	0.378	−0.058	−0.024	1.000	−0.512 *	−0.321	−0.128	−0.681 **	−0.512 *	0.188	−0.384
NDVI	0.445 **	−0.465 *	−0.099	−0.318	−0.512*	1.000	−0.479 *	0.841 **	0.262	1.000 **	−0.038	0.244
NDWI	0.040	0.006	0.224	0.272	−0.321	−0.479 *	1.000	−0.792 **	0.648 **	−0.479 *	−0.040	0.155
NDBI	0.406 *	−0.380	−0.185	−0.440*	−0.128	0.841 **	−0.792 **	1.000	−0.048	0.841 **	−0.075	0.064
NDSI	0.577	−0.466*	0.132	−0.106	−0.681 **	0.262	0.648 **	−0.048	1.000	0.262	−0.155	0.329
NDTI	0.445 *	−0.465 *	−0.099	−0.318	−0.512*	1.000 **	−0.479 *	0.841 **	0.262	1.000	−0.038	0.244
Distance of municipal wards from the old river course	−0.168	0.188	−0.106	0.165	0.188	−0.038	−0.040	−0.075	−0.155	−0.038	1.000	−0.782 **
Distance of municipal wards from the new river course	0.117	−0.029	0.234	−0.083	−0.384	0.244	0.155	0.064	0.329	0.244	−0.782 **	1.000

* Correlation is significant at the 0.05 level (2-tailed). <+ −0.3 0.3 to 0.7 >+ −0.7. ** Correlation is significant at the 0.01 level (2-tailed). **Source:** Calculated by the authors.

Table 8. Descriptive statistics of the selected variables (2015).

Variable	Mean	Std. Deviation (Standard Deviation)
NDFI2	0.3396	0.08503
Elevation	16.1529	2.64389
Slope	4.3016	2.45902
Flow Direction	34.4583	28.90502
Flow Distance	1.8811	2.01773
Flow Length Line Density	1.3057	0.40098
NDVI	−0.0867	0.02213
NDWI	0.2013	0.05387
NDBI	−0.0730	0.04289
NDSI	0.1306	0.03364
NDTI	−0.0867	0.02213
Distance of municipal wards from the old river course	1.4396	0.72325
Distance of municipal wards from the new river course	0.9729	0.62209
N (total municipal wards) = 24		

Source: Calculated by the authors.

Table 9. Model summary of the regression analysis (2015).

Model Summary [b]					
Model	**R**	**R Square**	**Adjusted R Square**	**Std. Error of the Estimate**	**Durbin–Watson**
	0.866 [a]	0.750	0.557	0.05659	2.513

[a.] Predictors: (constant), distance of municipal wards from the new river course, slope, NDWI, flow direction, flow length line density, elevation, flow distance, distance of municipal wards from the old river course, NDSI, NDTI. [b.] Dependent variable: NDFI2. **Source:** Calculated by the authors.

Table 10. Analysis of variance (ANOVA) of the regression analysis (2015).

ANOVA [a]					
Model	**Sum of Squares**	**df**	**Mean Square**	**F**	**Sig. (Significance)**
Regression	0.125	10	0.012	3.893	0.012 [b]
Residual	0.042	13	0.003		
Total	0.166	23			

[a.] Dependent variable: NDFI2. [b.] Predictors: (Constant), distance of municipal wards from the new river course, slope, NDWI, flow direction, flow length line density, elevation, flow distance, distance of municipal wards from the old river course, NDSI, NDTI. **Source:** Calculated by the authors.

A spatio-temporal variation of flood vulnerability has been identified in the present study for the years 2000 and 2015 (Figures 44 and 45). To determine the criteria weights of each variable, analytical hierarchy processes have been applied. Here, in the study, the coefficient of determinants (r square, non-negative value, Table 12) has been used to calculate the criteria weights of each of the variables. This is done by squaring the correlation coefficient (r-value) among the selected variables. A ward-wise composite flood vulnerability index has been computed for both years after the integration of the weights with the actual values. The proposed relationship between each of the factors and flood vulnerability is shown in Table 13 along with the criteria weights for 2000 and 2015, with the consistency index (CI) and consistency ratio (CR) being 0.156 and 0.101 in

2000 and 0.182 and 0.118 in 2015, respectively. Table 14 shows the ward-wise value of the composite flood vulnerability index (CFVI) in 2000 and 2015. In 2000, flood vulnerability was determined to be very high (0.37–0.99), high (0.26–0.36), moderate (0.17–0.25), low (0.064–0.16), and very low (0.0010–0.063) in the wards 10, 11, and 21; 8, 9, 13, and 14; 3, 4, 5, 6, 7, 12, and 15; 1, 17, 18, 19, and 22; and 2, 16, 20, 23, and 24, respectively (Figure 44). Similarly, in 2015, wards 7, 8, 9, and 10; 3, 4, 5, 6, and 21; 1, 2, 11, 12, 13, and 20; 144, 15, 16, 17, 18, and 19; and 22, 23, and 24 had very high (0.44–0.49), high (0.34–0.43), moderate (0.20–0.33), low (0.081–0.09), and very low (0.0010–0.080) flood vulnerability, respectively (Figure 45). Figures 46 and 47 show the isoline zones of the composite flood vulnerability index in Nabadwip Municipality (2000 and 2015) and Figures 48–54 show the normal probability plots, the relationship between regression standardized predicted values (ZPR) and NDFI2, the plotted map of ZPR, the frequency distribution of regression standardized residuals (ZRE), the relationship between regression ZRE and NDFI2, and the plotted map of regression ZRE, respectively.

Table 11. Coefficients of the regression analysis (2015).

Coefficients [a]									
	Unstandardized Coefficients		Standardized Coefficients			95.0% Confidence Interval for B		Collinearity Statistics	
Model	B	Std. Error	Beta	t	Sig.	Lower Bound	Upper Bound	Tolerance	VIF (Variance Inflation Factor)
(Constant)	0.455	0.199		2.288	0.040	0.025	0.885		
Elevation	0.024	0.008	0.748	2.966	0.011	0.007	0.042	0.303	3.299
Slope	0.017	0.013	0.485	1.265	0.228	−0.012	0.045	0.131	7.624
Flow Direction	0.000	0.001	0.166	0.861	0.405	−0.001	0.002	0.518	1.931
Flow Distance	−0.015	0.010	−0.360	−1.458	0.169	−0.038	0.007	0.315	3.173
Flow Length Line Density	0.054	0.060	0.254	0.900	0.384	−0.076	0.183	0.241	4.145
NDWI	4.599	1.029	2.913	4.470	0.001	2.376	6.821	0.045	22.055
NDSI	−5.790	1.291	−2.291	−4.484	0.001	−8.580	−3.001	0.074	13.554
NDTI	6.476	2.267	1.685	2.857	0.013	1.579	11.373	0.055	18.067
Distance of municipal wards from the old river course	−0.106	0.046	−0.903	−2.304	0.038	−0.206	−0.007	0.125	7.971
Distance of municipal wards from the new river course	−0.093	0.057	−0.677	−1.634	0.126	−0.215	0.030	0.112	8.920
[a.] Dependent Variable: NDFI2									
Excluded Variables [a]									
Model						Collinearity Statistics			
	Beta In	t	Sig.	Partial Correlation	Tolerance	VIF		Minimum Tolerance	
NDVI	.[b]	.	.	.	0.000	.		0.000	
NDBI	15.410 [b]	0.957	0.358	0.266	0.00007472	13382.683		0.00004458	
[a.] Dependent Variable: NDFI2									

[b.] Predictors in the model: (constant), distance of municipal wards from the new river course, slope, NDWI, flow direction, flow length line density, elevation, flow distance, distance of municipal wards from the old river course, NDSI, NDTI

Source: Calculated by the authors.

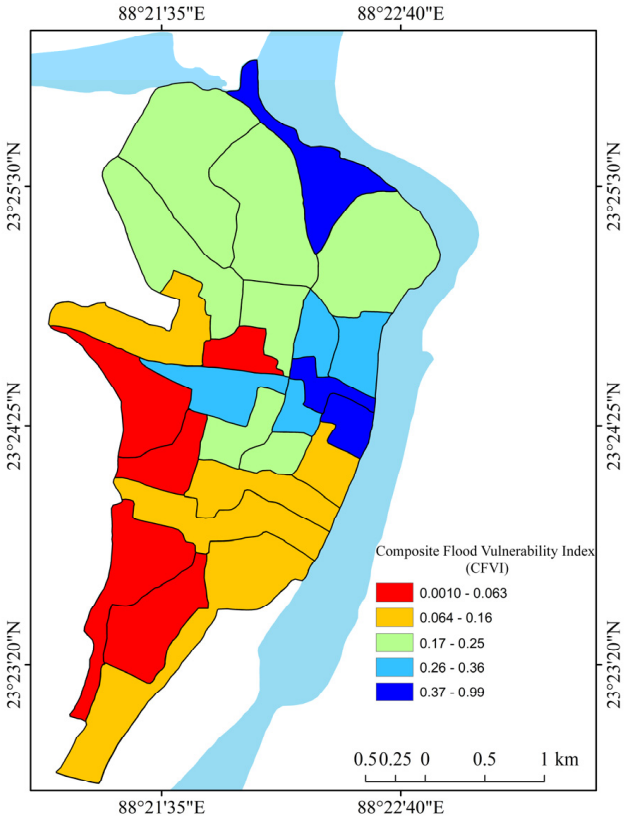

Figure 44. Composite flood vulnerability index of Nabadwip Municipality (2000).

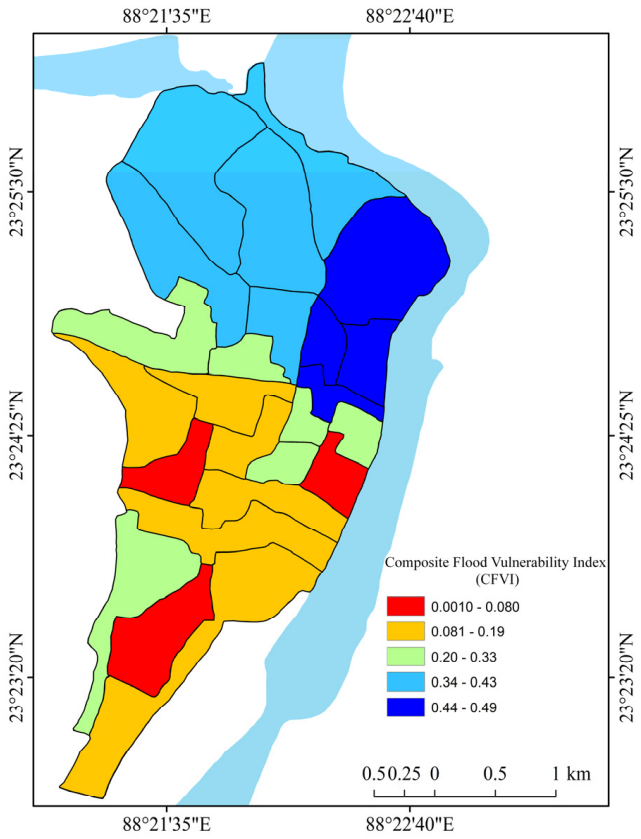

Figure 45. Composite flood vulnerability index of Nabadwip Municipality (2015).

Table 12. Coefficient of determinants (assigned weights of MCDM) of the selected indicators of flood vulnerability (2000 and 2015).

R Square (2000)	**Elevation**	**Slope**	**Flow Direction**	**Flow Distance**	**Flow Length Line Density**	**NDVI**	**NDWI**	**NDBI**	**NDSI**	**NDTI**	**Distance of Municipal Wards from the Old River Course**	**Distance of Municipal Wards from the New River Course**
Elevation	1.000	0.007	0.004	0.135	0.077	0.014	0.001	0.001	0.004	0.023	0.028	0.014
Slope	0.007	1.000	0.006	0.196	0.000	0.003	0.008	0.008	0.000	0.000	0.252	0.158
Flow Direction	0.004	0.006	1.000	0.083	0.020	0.008	0.003	0.003	0.004	0.002	0.019	0.060
Flow Distance	0.135	0.196	0.083	1.000	0.045	0.000	0.005	0.005	0.002	0.007	0.003	0.088
Flow Length Line Density	0.077	0.000	0.020	0.045	1.000	0.008	0.001	0.001	0.005	0.007	0.018	0.085
NDVI	0.014	0.003	0.008	0.000	0.008	1.000	0.457	0.457	0.215	0.594	0.064	0.149
NDWI	0.001	0.008	0.003	0.005	0.001	0.457	1.000	1.000	0.812	0.516	0.114	0.084
NDBI	0.001	0.008	0.003	0.005	0.001	0.457	1.000	1.000	0.812	0.516	0.114	0.084
NDSI	0.004	0.000	0.004	0.002	0.005	0.215	0.812	0.812	1.000	0.476	0.061	0.018
NDTI	0.023	0.000	0.002	0.007	0.007	0.594	0.516	0.516	0.476	1.000	0.055	0.107
Distance of municipal wards from the old river course	0.028	0.252	0.019	0.003	0.018	0.064	0.114	0.114	0.061	0.055	1.000	0.612
Distance of municipal wards from the new river course	0.014	0.158	0.060	0.088	0.085	0.149	0.084	0.084	0.018	0.107	0.612	1.000
R square (2015)	Elevation	Slope	Flow Direction	Flow Distance	Flow Length Line Density	NDVI	NDWI	NDBI	NDSI	NDTI	Distance of municipal wards from the old river course	Distance of municipal wards from the new river course
Elevation	1.000	0.402	0.060	0.067	0.092	0.198	0.002	0.165	0.333	0.198	0.028	0.014
Slope	0.402	1.000	0.164	0.365	0.143	0.216	0.000	0.144	0.217	0.216	0.035	0.001
Flow Direction	0.060	0.164	1.000	0.010	0.003	0.010	0.050	0.034	0.017	0.010	0.011	0.055
Flow Distance	0.067	0.365	0.010	1.000	0.001	0.101	0.074	0.194	0.011	0.101	0.027	0.007
Flow Length Line Density	0.092	0.143	0.003	0.001	1.000	0.262	0.103	0.016	0.464	0.262	0.035	0.147

Table 12. *Cont.*

R Square (2000)	Elevation	Slope	Flow Direction	Flow Distance	Flow Length Line Density	NDVI	NDWI	NDBI	NDSI	NDTI	Distance of Municipal Wards from the Old River Course	Distance of Municipal Wards from the New River Course
NDVI	0.198	0.216	0.010	0.101	0.262	1.000	0.229	0.707	0.069	1.000	0.001	0.060
NDWI	0.002	0.000	0.050	0.074	0.103	0.229	1.000	0.627	0.420	0.229	0.002	0.024
NDBI	0.165	0.144	0.034	0.194	0.016	0.707	0.627	1.000	0.002	0.707	0.006	0.004
NDSI	0.333	0.217	0.017	0.011	0.464	0.069	0.420	0.002	1.000	0.069	0.024	0.108
NDTI	0.198	0.216	0.010	0.101	0.262	1.000	0.229	0.707	0.069	1.000	0.001	0.060
Distance of municipal wards from the old river course	0.028	0.035	0.011	0.027	0.035	0.001	0.002	0.006	0.024	0.001	1.000	0.612
Distance of municipal wards from the new river course	0.014	0.001	0.055	0.007	0.147	0.060	0.024	0.004	0.108	0.060	0.612	1.000

Source: Calculated by the authors.

Table 13. Criteria weights of the MCDM process and proposed relationship of the indicators with flood vulnerability (2000 and 2015).

Variable	Criteria Weight (2000)	Criteria Weight (2015)	Presumption of the Relationship with Flood Vulnerability
Elevation	0.11	0.21	-
Slope	0.14	0.24	-
Flow Direction	0.10	0.12	+
Flow Distance	0.13	0.16	-
Flow Length Line Density	0.11	0.21	+
NDVI	0.25	0.32	-
NDWI	0.33	0.23	+
NDBI	0.33	0.30	+
NDSI	0.28	0.23	+
NDTI	0.28	0.32	+
Distance of municipal wards from the old river course	0.19	0.15	+
Distance of municipal wards from the new river course	0.20	0.17	-
	Consistency Index (CI) = 0.156 Consistency Ratio (CR) = 0.101	Consistency Index (CI) = 0.182 Consistency Ratio (CR) = 0.118	

Source: Calculated by the authors.

Random Index (*RI*)												
n	1	2	3	4	5	6	7	8	9	10	11	12
RI	0.00	0.00	0.52	0.89	1.11	1.25	1.35	1.40	1.45	1.49	1.51	1.54

Source: [73].

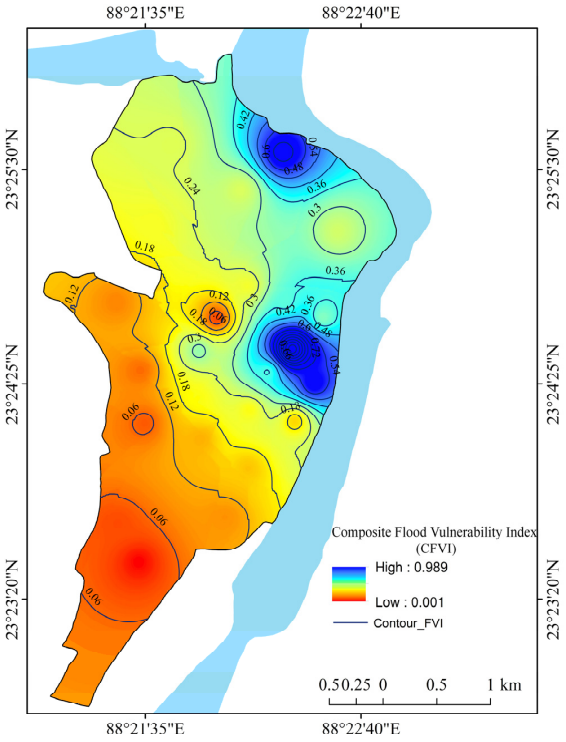

Figure 46. Isoline of CFVI (2000).

Table 14. Composite flood vulnerability index (CFVI) (2000 and 2015) and composite Ibrahim index (CIb) (2015) of the wards of Nabadwip Municipality.

Ward	Latitude	Longitude	CFVI (2000)	CFVI (2015)	CIb (2015)
1	23.41379929	88.3572998	0.086	0.292	24.00
2	23.41250038	88.36569977	0.033	0.322	53.63
3	23.41519928	88.36820221	0.208	0.366	34.56
4	23.42040062	88.36049652	0.204	0.386	25.51
5	23.42700005	88.36199951	0.235	0.408	21.88
6	23.42320061	88.36769867	0.244	0.429	27.74
7	23.4197998	88.37580109	0.253	0.451	22.90
8	23.41259956	88.37460327	0.329	0.475	24.34
9	23.41390038	88.37139893	0.352	0.485	36.87
10	23.40990067	88.37200165	0.991	0.491	40.27
11	23.40699959	88.37380219	0.595	0.327	36.75
12	23.40480042	88.36849976	0.194	0.234	41.65
13	23.40800095	88.36990356	0.358	0.239	26.85
14	23.40979958	88.36419678	0.313	0.190	32.80
15	23.40579987	88.3640976	0.194	0.141	36.32
16	23.40810013	88.35929871	0.063	0.123	33.25
17	23.40229988	88.36440277	0.123	0.157	31.93
18	23.39990044	88.36830139	0.140	0.175	31.09
19	23.39579964	88.36640167	0.096	0.193	30.25
20	23.39520073	88.35739899	0.036	0.252	30.22
21	23.42639923	88.37120056	0.624	0.398	25.90
22	23.40390015	88.37220001	0.157	0.080	35.08
23	23.40369987	88.35970306	0.048	0.003	44.66
24	23.39209938	88.35919952	0.001	0.001	24.17

Source: Calculated by the authors.

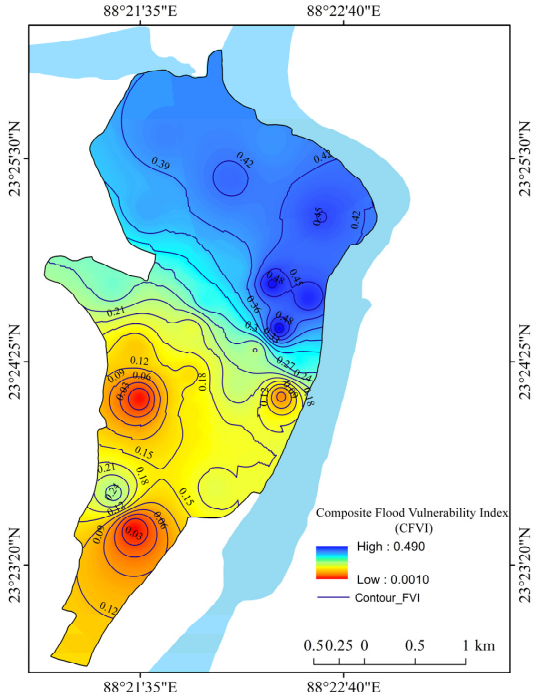

Figure 47. Isoline of CFVI (2015).

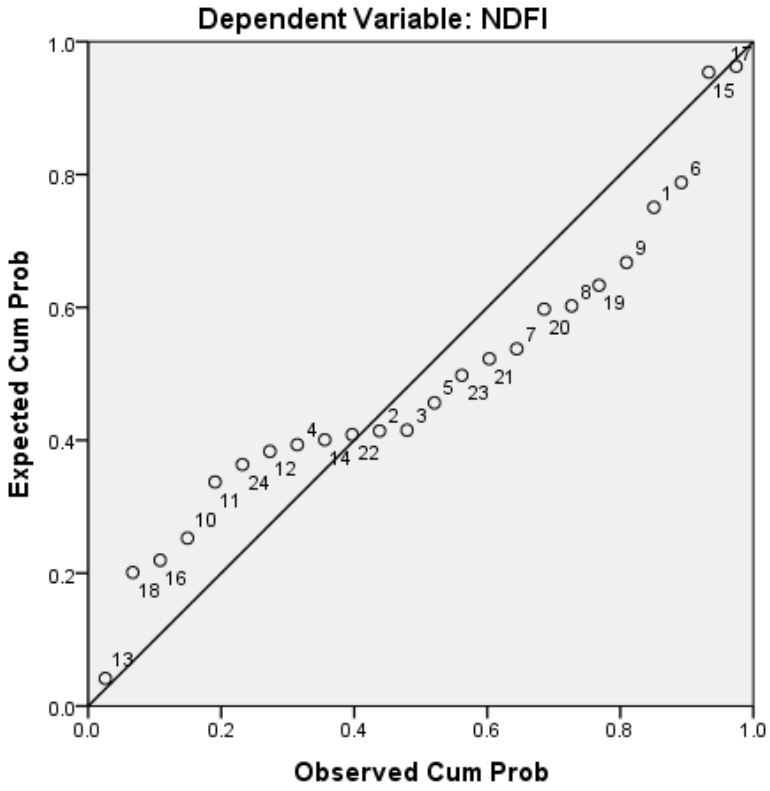

Figure 48. The normal p–p plot of regression ZRE.

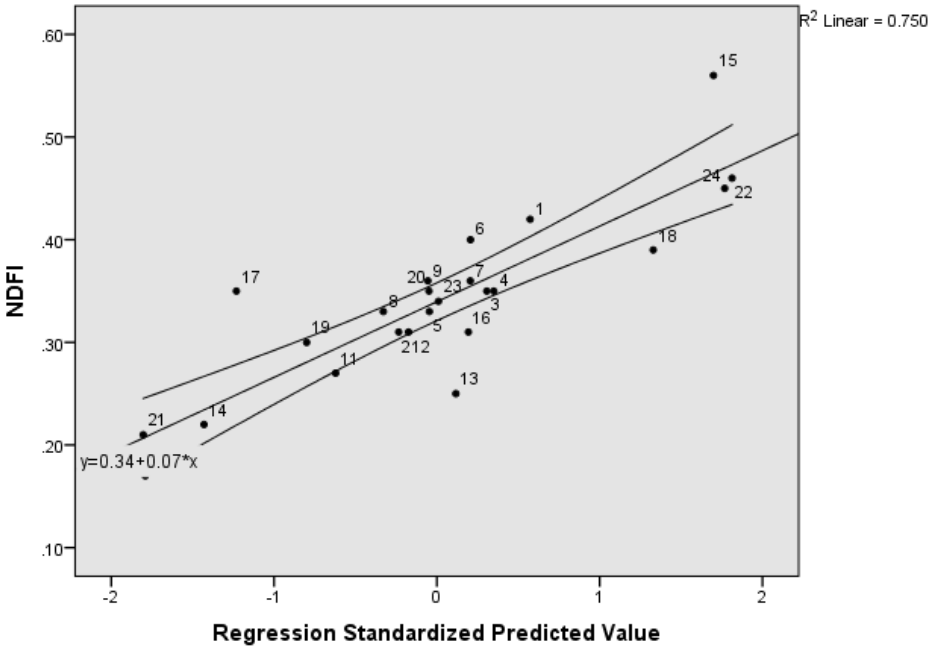

Figure 49. Relationship between regression ZPR and NDFI2.

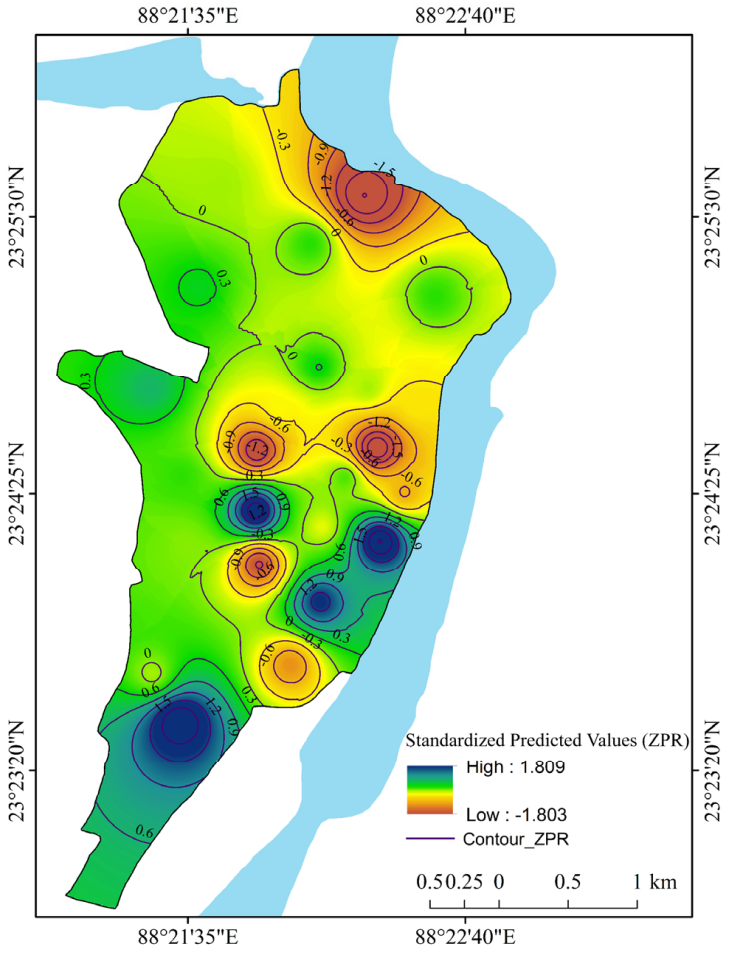

Figure 50. Plots of regression ZPR (2015).

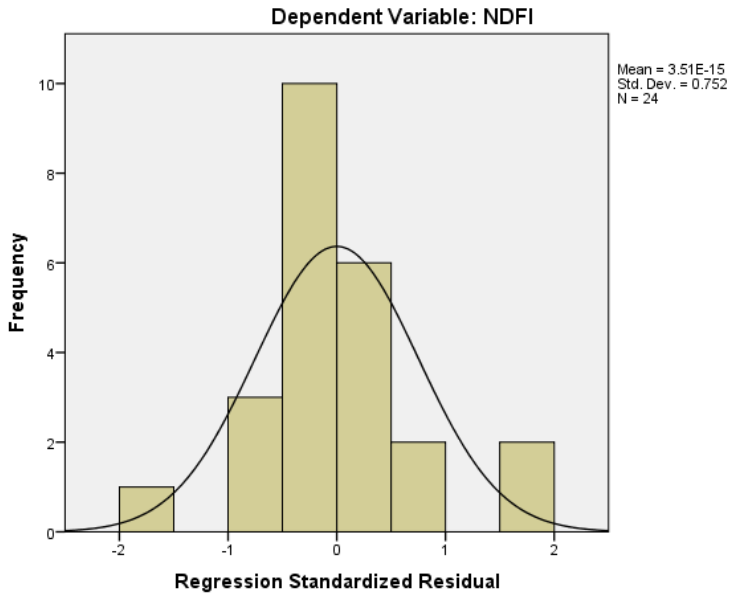

Figure 51. Frequency distribution of regression ZRE.

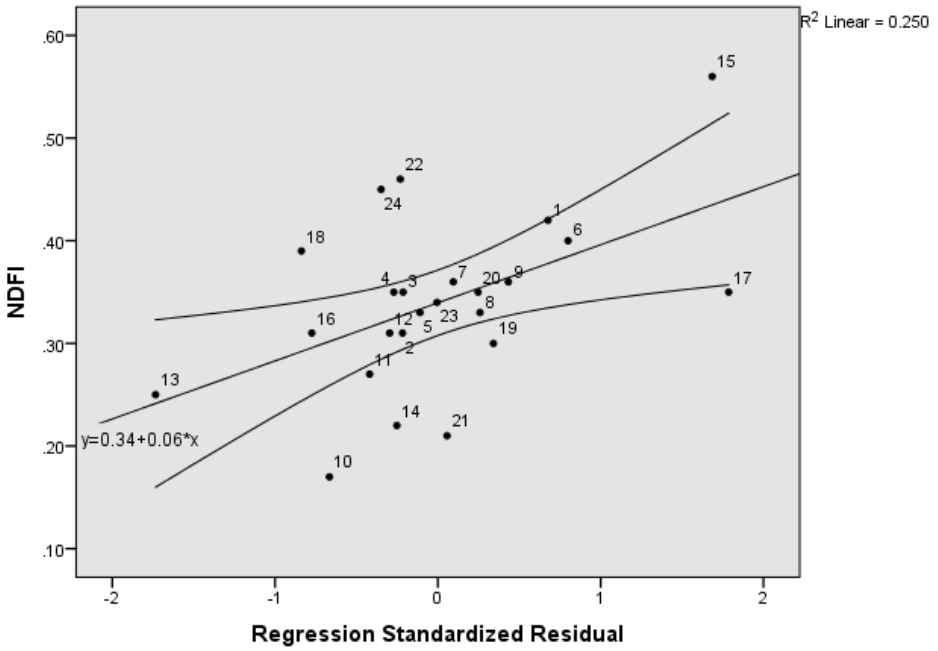

Figure 52. Relationship between regression ZRE and NDFI2.

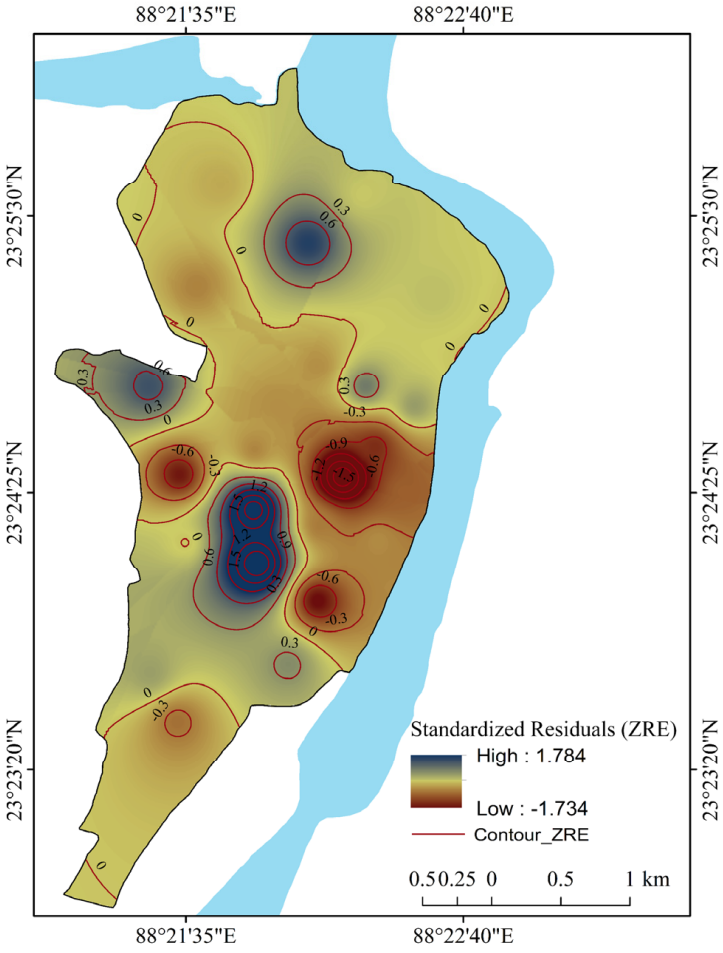

Figure 53. Plots of regression ZRE (2015).

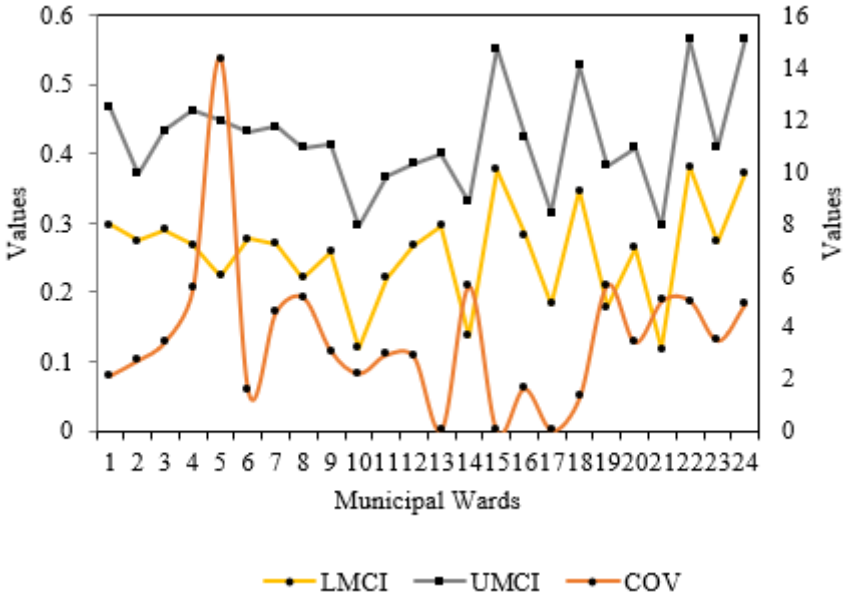

Figure 54. Plotted graph of Lower Mean Confidence Interval (LMCI), Upper Mean Confidence Interval (UMCI), and Covariance (COV) of regression analysis.

4.3. Relationship between Urban Development and Flood Vulnerability

The socio-economic and urban amenity situation is variedly distributed in the wards of the study area. Figures 55–59 show the ward-wise distribution of households, SC population, ST population, literates, and workers per thousand population in 2015. In 2015, the composite Ibrahim index (Ib) of the socio-economic status of urban development was high in wards 2, 10, 12, and 23 (the CIb value is 36.88–53.63); moderately high (33.26–36.87) in wards 3, 9, 11, 15, and 22; moderate (30.23–33.25) in wards 14, 16, 17, 18, and 19; moderately low (24.35–30.22) in wards 4, 6, 13, 20, and 21; and low (21.88–24.34) in wards 1, 5, 7, 8 and 24 (Figure 60). Figure 61 shows the overlapping layer of isolines of the composite flood vulnerability index on the interpolated inverse distance weight (IDW) zones of the composite Ibrahim index. The relationship between urban development and flood vulnerability is illustrated in Figure 62. Here, a negative relationship has been identified between the flood vulnerability index and the composite Ibrahim index of the 24 wards of Nabadwip Municipality in 2015 (the r square value is 0.0368, so a 1-unit increase in the CIb results in a 3.68% decrease in the CFVI). In general, highly developed areas within the municipality have a low risk of flooding, but real-world examples and current research show that some of the developing wards of Nabadwip Municipality are particularly vulnerable to flooding.

The findings of the hypothesis testing are presented in Table 15. Here, the population means of the CFVI and CIb are 0.27575 and 32.1925, respectively. The standard deviation values of the two variables are 0.1494309 and 7.72409, respectively. The differences between the two population means and standard errors have been measured as −31.91675 and 1.576968, respectively. As it is presumed that the difference = mean (CFVI) − mean (CIb) where H_0: difference = 0, the estimated t value is −20.2393 (Welch's degrees of freedom = 23.0187) with a 0.05 significance level. The t value has been calculated by dividing the combined mean by the combined standard error; that is, −31.91675/1.576968 = −20.2393. Based on the alternative hypothesis, Ha: diff! = 0, the *p*-value is less than 0.05 (Pr (|T| > |t|) = 0.0000). This proves that the difference in means is statistically significantly different from zero (two-tailed test). Consequently, the alternative hypothesis has been accepted with the rejection of the null hypothesis. Among the other two alternative hypotheses (Ha: diff < 0 and Ha: diff > 0) of the one-tailed test, the former is statistically significant as $p < 0.05$ (Pr (T < t) = 0.0000), and the latter is not statistically significant as $p > 0.05$ (Pr (T > t) = 1.0000). Therefore, it can be specified that the variance of the composite Ibrahim index of socio-

economic development is greater than the variance of the composite flood vulnerability index in the study area.

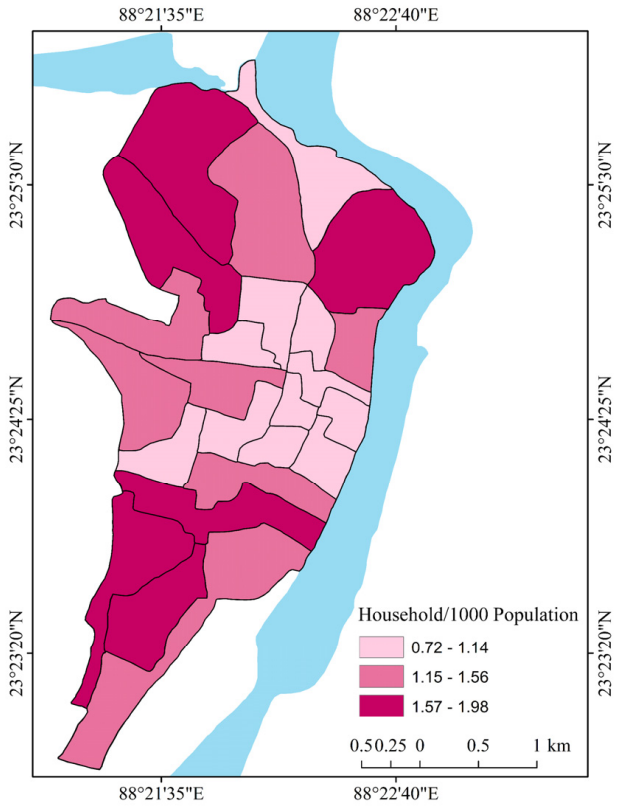

Figure 55. Ward-wise distribution of households/1000 population in Nabadwip Municipality (2011).

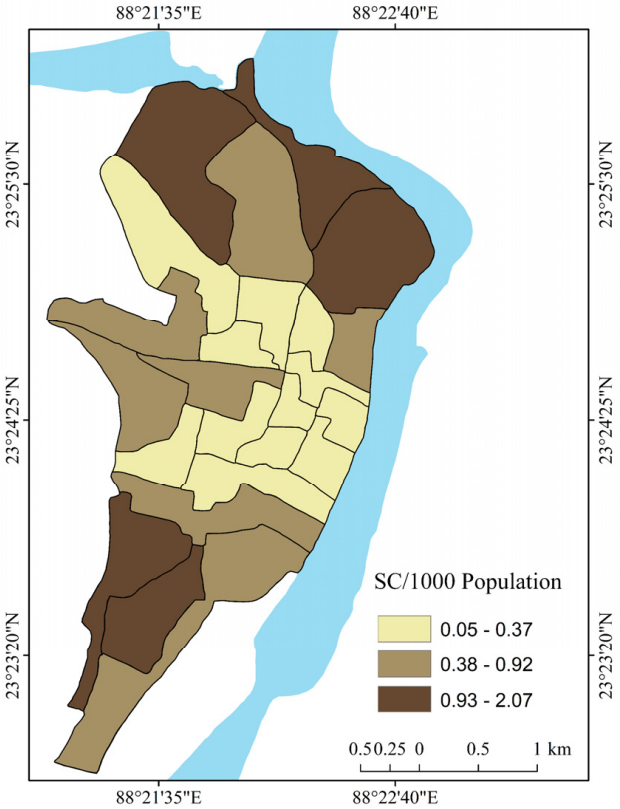

Figure 56. Ward-wise distribution of SC/1000 population in Nabadwip Municipality (2011).

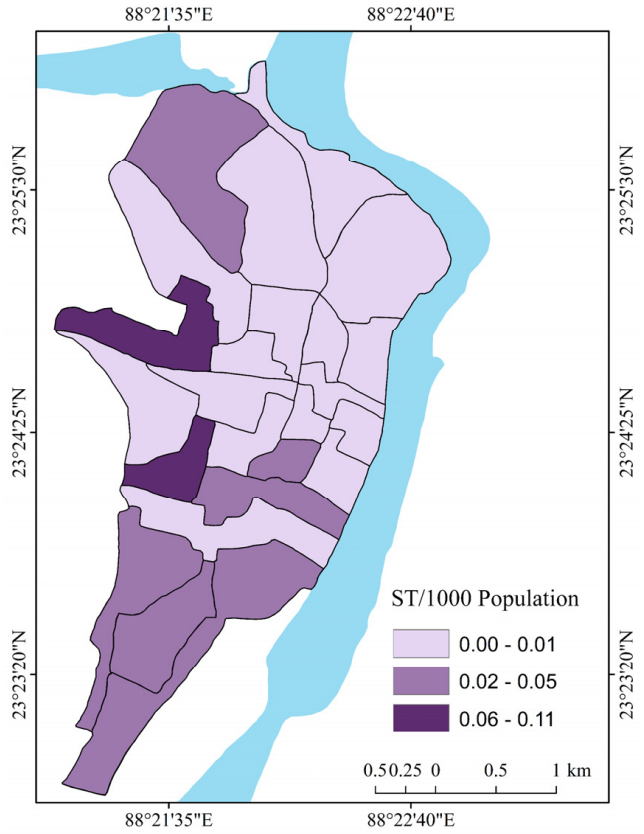

Figure 57. Ward-wise distribution of ST/1000 population in Nabadwip Municipality (2011).

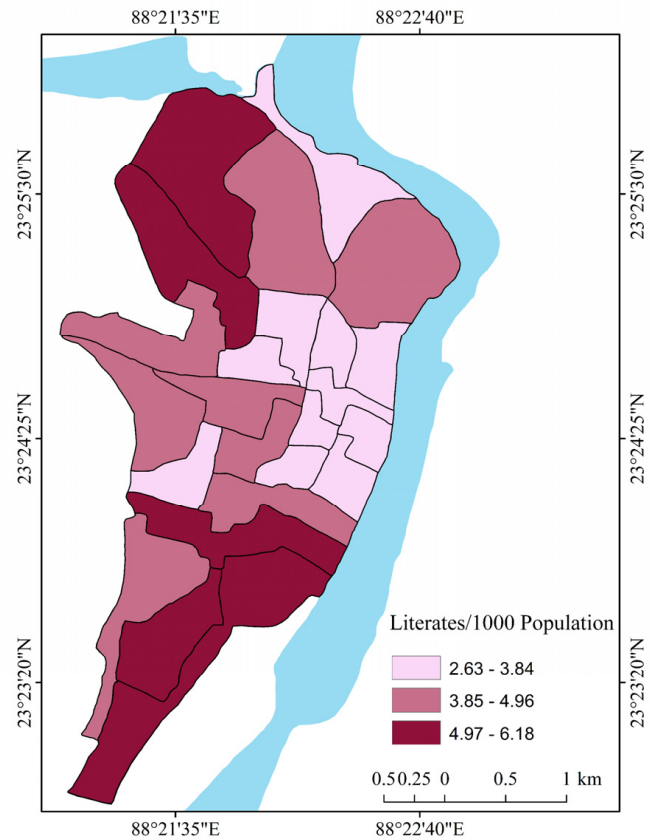

Figure 58. Ward-wise distribution of literates/1000 population in Nabadwip Municipality (2011).

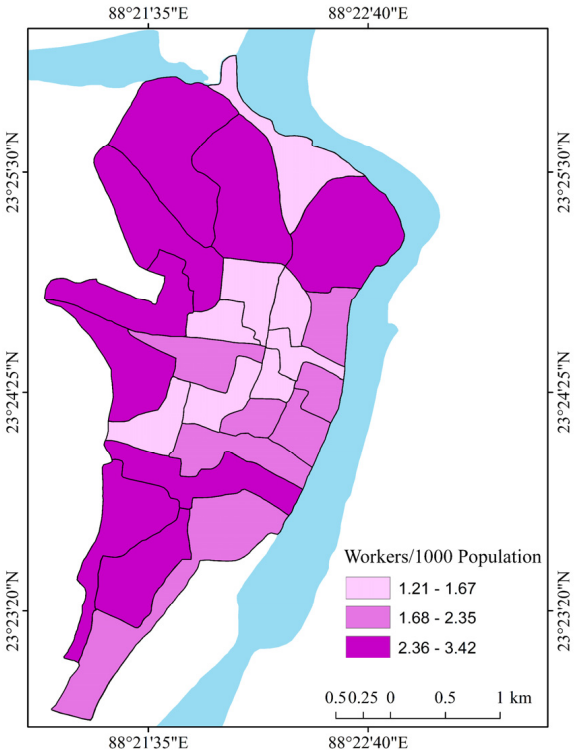

Figure 59. Ward-wise distribution of workers/1000 of the population in Nabadwip Municipality (2011).

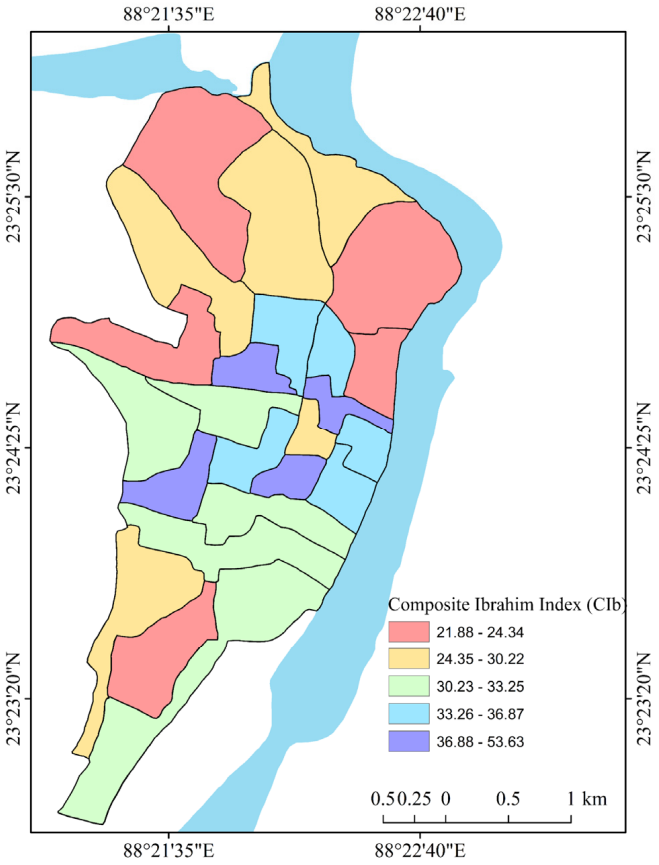

Figure 60. Ward-wise composite Ibrahim index of development in Nabadwip Municipality (2015).

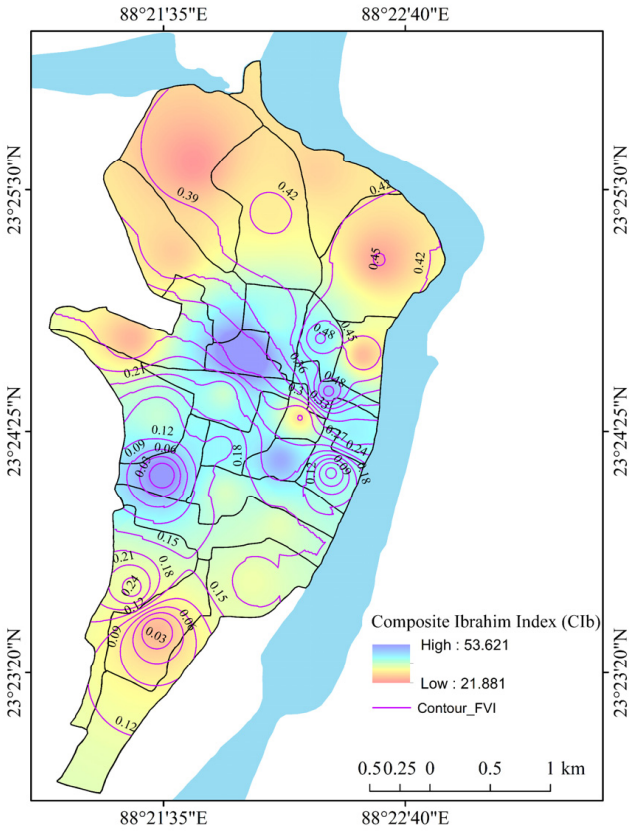

Figure 61. Comparison between ward-wise composite Ibrahim index of development and composite flood vulnerability index in Nabadwip Municipality (2015).

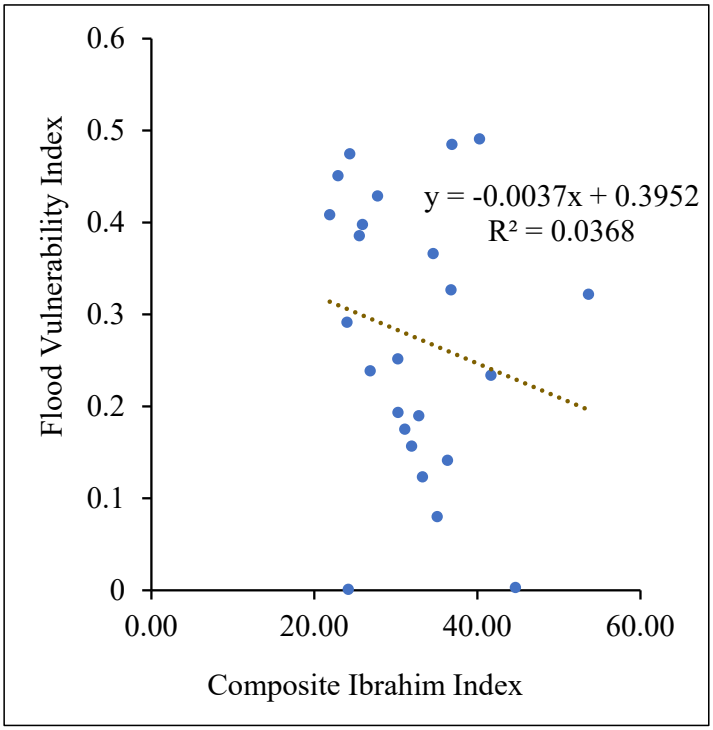

Figure 62. Relationship between composite Ibrahim index of development and composite flood vulnerability index in Nabadwip Municipality (2015).

Table 15. Results of Hypothesis testing.

Two-Sample *t*-Test with Unequal Variances						
Variable	**Obs**	**Mean**	**Std. Err.**	**Std. Dev.**	**95% Conf.**	**Interval**
CFVI (2015)	24	0.27575	0.0305024	0.1494309	0.2126509	0.3388491
CIb (2015)	24	32.1925	1.576673	7.72409	28.9309	35.4541
combined	48	16.23413	2.454992	17.00868	11.29532	21.17293
diff		−31.91675	1.576968		−35.17881	−28.65469
diff = mean (CFVI) − mean (CIb) t = −20.2393 Ho: diff = 0 Welch's degrees of freedom = 23.0187						
Ha: diff < 0 Ha: diff! = 0 Ha: diff > 0 Pr (T < t) = 0.0000 Pr (|T| > |t|) = 0.0000 Pr (T > t) = 1.0000						

Here, Obs is the number of valid (non-missing) observations used in calculating the t-test, Std. Err. is the standard error, Std. Dev. is the standard deviation, Conf. Interval is the confidence interval, diff denotes difference, Ho = null hypothesis, Ha = alternative hypothesis, and Pr denotes predicted.

Source: Calculated by the authors.

5. Major Findings, Discussion, and Policy Suggestions

The current study examines and elucidates rainfall variability, factors that contribute to flooding, flood vulnerability and its spatio-temporal dimension, correlations among the predictors of floods, relationships between the factors of flood vulnerability and the normalized difference flood index, and the relationship between urban development and flood vulnerability. The monthly and daily rainfall patterns between 2000 and 2015 show that the monsoon season is characterized by exceptionally heavy rainfall caused by cyclonic depressions. The majority of Nabadwip Municipality and surrounding areas experienced significant flooding due to the influence of heavy rainfall and a high discharge within a short period. In comparison to the other months during the 2015 monsoon season, July was a moderately humid month according to the SPI values. In 2000, a flood situation characterized by a high water level in this municipality's wards had a devastating impact on both property and human lives. The selected physical factors of flood vulnerability had a positive or negative impact on flood affectivity. The flood index increased with increasing elevation, slope, flow direction, flow length, line density, NDWI, and NDTI, whereas it decreased with increasing flow distance, NDSI, the distance of municipal wards from the old river course, and the distance of municipal wards from the new river course. A highly concretized relief and slope can increase the flood vulnerability in the study area, whereas increasing stream flow direction and flow length line density naturally increased the flood vulnerability when they were in peak form during the monsoon. The main channel of the Bhagirathi-Hugli could no longer withstand the unprecedented pressure of heavy discharge during stormy rainfall, which led to flood situations. The high value of the water index also indicated higher flood conditions and high river turbidity indicated an increasing amount of siltation into the river. Municipality wards that are located closer to the new river course are typically more at risk than those that are farther away. The flood situation between 2000 and 2015 exhibited a substantial change. The number of very high, moderate, and very low vulnerability wards had decreased compared to 2000, while high and low vulnerability wards had increased. Figure 48 depicts the relationship between the observed and expected cumulative probability distribution of the computed residuals of the relationship between NDFI2 and its predictors. The points for the corresponding wards 13, 14, 15, and 17 are positioned here on the line of equality, while the others are positioned far from it. The values away from the equality line indicate that the anticipated likelihood of a flood is either too high or too low (high in the case of the points below the line, low in the case of the points above the line). In terms of the best fit, the mean occurrences pertain

to the points that are exactly positioned on the line (Figure 48). The flood vulnerability indices have been validated using the ROC-AUC analysis (Figures 63 and 64). The overall accuracy of the AUC was 73.9% in 2000 and 77.5% in 2015. Thus, the model is validated and further acceptable. In 2015, the sensitivity and specificity rates increased. Better performance is indicated by classifiers that provide curves that are closer to the top-left corner. The values of the area of fitted ROCs are good and within an acceptable range, varying from 0.7–0.8 in 2000 to 0.8–0.9 in 2015. The variations have consequences for the changes to the distribution facilities for urban amenities and the socio-economic conditions of the residents of Nabadwip Municipality. In general, the wards exhibited moderately high and higher socio-economic development where the vulnerability to flooding was low. Contrarily, some of the underdeveloped wards located relatively in a high-elevation area of the city fringe showed less vulnerability to flooding occurrences than some of the developed wards located at low elevations and closer to the city center. The results of the hypothesis test also revealed a significant association between socio-economic development and flood vulnerability, but the variability of socio-economic development is greater than the conditions of flood vulnerability in Nabadwip Municipality. Further research on this municipality area is usually required in this context of a dichotomous situation. This study takes into account flood vulnerability mitigation measures. To lessen the 'most adverse' effects of flood hazards on the physical and anthropogenic environment, 'flood prevention', 'mitigation strategies', and improved resilience are necessary [93]. In this regard, a strengths, weaknesses, opportunities, challenges (SWOC) analysis was conducted to determine the main strengths, weaknesses, opportunities, and challenges related to urban development and flood vulnerability in the Nabadwip Municipality area. Strengths, weaknesses, opportunities, and threats (SWOT) analyses had been performed in earlier literature for a range of purposes. The SWOT of Dutch water storage areas were analyzed for flood prevention and flood risk management [94]. The researchers also used SWOT analysis in some other studies [95,96] they conducted on flood preparedness, mitigation, and management. Based on participant observations, the present study has identified two important strengths, four weaknesses, five opportunities, and five challenges of urban development and flood vulnerability in Nabadwip Municipality. Based on their priorities for urban development and flood vulnerability, the SWOC have been ranked separately (Table 16). A SWOC matrix has been generated in Table 17 to show the combinations of greater challenges and weaknesses as well as better opportunities and strengths. The Weakness 1, Challenge 1 (W1C1), and Opportunity 2, Strength 1 (O2S1) combinations are the most influential and effective strategies to combat floods. The proper reconstruction of sewage systems along with the dredging of river silt would be effective in the Nabadwip Municipality area to minimize flood risks and vulnerabilities. In addition, well-connected roads and railways adjacent to wide tourism activity will continue to initiate better employment opportunities in the study area, which will drive urban development strategies in a more prosperous way.

Table 16. Selected strengths, weaknesses, opportunities, and challenges (SWOC) in Nabadwip Municipality area.

	SWOC	Code	Relative Importance (Rank)
	Strengths		
1	Better road and railway connectivity.	S1	1
2	A significant number of water bodies.	S2	2
	Weaknesses		
1	Unstructured sewage system.	W1	1
2	Unplanned built-up areas.	W2	4
3	Roadways are not properly maintained.	W3	3
4	Health facilities are inadequate.	W4	2

Table 16. *Cont.*

	SWOC	Code	Relative Importance (Rank)
	Opportunities		
1	Better agricultural production in fringe areas.	O1	5
2	International importance on tourism.	O2	1
3	Building up a comprehensive urban development.	O3	4
4	Participation of local people in flood management.	O4	3
5	New employment opportunities through the flood management system.	O5	2
	Challenges		
1	River dredging has not been performed.	C1	1
2	Resettlement is problematic during the flood.	C2	4
3	Inadequate distribution of flood relief.	C3	3
4	Indigent damage control network.	C4	5
5	A large number of poverty-stricken people.	C5	2

Source: The authors.

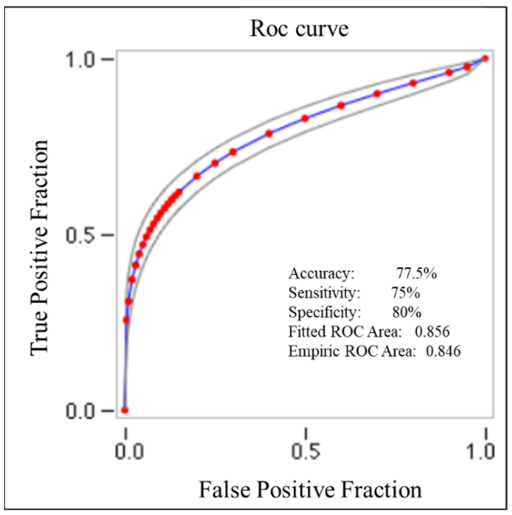

Figure 63. Validation of composite flood vulnerability index using ROC-AUC (2000).

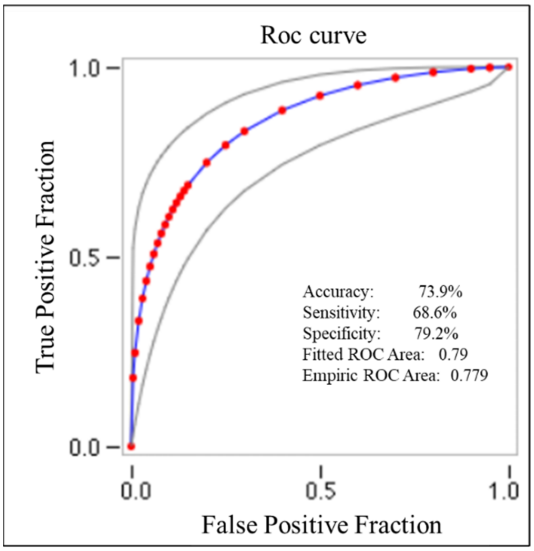

Figure 64. Validation of composite flood vulnerability index using ROC-AUC (2015).

Table 17. SWOC matrix.

Matrix	Strengths		Weaknesses				Opportunities					Challenges				
	S1	S2	W1	W2	W3	W4	O1	O2	O3	O4	O5	C1	C2	C3	C4	C5
S1	S1S1	S1S2	S1W1	S1W2	S1W3	S1W4	S1O1	S1O2	S1O3	S1O4	S1O5	S1C1	S1C2	S1C3	S1C4	S1C5
S2	S2S1	S2S2	S2W1	S2W2	S2W3	S2W4	S2O1	S2O2	S2O3	S2O4	S2O5	S2C1	S2C2	S2C3	S2C4	S2C5
W1	W1S1	W1S2	W1W1	W1W2	W1W3	W1W4	W1O1	W1O2	W1O3	W1O4	W1O5	W1C1	W1C2	W1C3	W1C4	W1C5
W2	W2S1	W2S2	W2W1	W2W2	W2W3	W2W4	W2O1	W2O1	W2O1	W2O1	W2O1	W2C1	W2C2	W2C3	W2C4	W2C5
W3	W3S1	W3S2	W3W1	W3W2	W3W3	W3W4	W2O1	W2O1	W2O1	W2O1	W2O1	W3C1	W3C2	W3C3	W3C4	W3C5
W4	W4S1	W4S2	W4W1	W4W2	W4W3	W4W4	W4O1	W4O2	W4O3	W4O4	W4O5	W4C1	W4C2	W4C3	W4C4	W4C5
O1	O1S1	O1S2	O1W1	O1W2	O1W3	O1W4	O1O1	O1O2	O1O3	O1O4	O1O5	O1C1	O1C2	O1C3	O1C4	O1C5
O2	O2S1	O2S2	O2W1	O2W2	O2W3	O2W4	O2O1	O2O2	O2O3	O2O4	O2O5	O2C1	O2C2	O2C3	O2C4	O2C5
O3	O3S1	O3S2	O3W1	O3W2	O3W3	O3W4	O3O1	O3O2	O3O3	O3O4	O3O5	O3C1	O3C2	O3C3	O3C4	O3C5
O4	O4S1	O4S2	O4W1	O4W2	O4W3	O4W4	O4O1	O4O2	O4O3	O4O4	O4O5	O4C1	O4C2	O4C3	O4C4	O4C5
O5	O5S1	O5S2	O5W1	O5W2	O5W3	O5W4	O5O1	O5O2	O5O3	O5O4	O5O5	O5C1	O5C2	O5C3	O5C4	O5C5
C1	C1S1	C1S2	C1W1	C1W2	C1W3	C1W4	C1O1	C1O2	C1O3	C1O4	C1O5	C1C1	C1C2	C1C3	C1C4	C1C5
C2	C2S1	C2S2	C2W1	C2W2	C2W3	C2W4	C2O1	C2O2	C2O3	C2O4	C2O5	C2C1	C2C2	C2C3	C2C4	C2C5
C3	C3S1	C3S2	C3W1	C3W2	C3W3	C3W4	C3O1	C3O2	C3O3	C3O4	C3O5	C3C1	C3C2	C3C3	C3C4	C3C5
C4	C4S1	C4S2	C4W1	C4W2	C4W3	C4W4	C4O1	C4O2	C4O3	C4O4	C4O5	C4C1	C4C2	C4C3	C4C4	C4C5
C5	C5S1	C5S2	C5W1	C5W2	C5W3	C5W4	C5O1	C5O2	C5O3	C5O4	C5O5	C5C1	C5C2	C5C3	C5C4	C5C5

Source: The authors.

6. Conclusions

The urban flood situation disastrously impacts the properties, lives, and livelihoods of urban residents. In this era of climate change, severe floods have occurred in the world's largest urban areas as a result of rapid urbanization and urban encroachment. Nabadwip Municipality, the present study area, is also a significant urban body in the Indian state of West Bengal. In the study area, the frequency of floods is influenced by several physical factors. Among them, the most useful and significant variables were flow length and line density, NDWI and NDSI, the distance of municipal wards from the old river course, and the distance of municipal wards from the new river course. The municipality area had experienced impairing floods multiple times. The significant flooding that occurred between 2000 and 2020 was devastating in the years 2000 and 2015. Floods in Nabadwip and the surrounding areas were severely impacted by seasonal rainfall variability and high daily rainfall during the monsoon season. In the years 2000 and 2015, the normalized difference flood index indicated a variety of relationships with the predictor variables. According to the composite Ibrahim index of socio-economic developmental status and the composite flood vulnerability index, some developing countries were less vulnerable to flooding than others, and the majority of underdeveloped countries were more vulnerable. Despite this, it became apparent that some of the developed municipal wards located closer to the city's center were more susceptible to flooding. The implementation of flood recovery, resilient management, awareness, and capacity building, along with the proper maintenance of sewage systems, river dredging, the integration of structured urban planning, and employment generation, are required to mitigate and manage the flood effects in the studied municipality area in the future.

Author Contributions: Conceptualization, B.K.M. and T.B.; Methodology, B.K.M. and T.B.; Software, B.K.M. and T.B.; Validation, B.K.M., T.B., K.A., M.S.F. and S.P.; Formal Analysis, T.B. and B.K.M.; Investigation, B.K.M. and T.B.; Resources, B.K.M. and T.B.; Data Curation, T.B. and B.K.M.; Writing—Original Draft Preparation, T.B. and B.K.M.; Writing—Review and Editing, B.K.M., T.B., K.A., M.S.F. and S.P.; Visualization, T.B.; Supervision, B.K.M.; Project Administration, B.K.M.; Funding Acquisition, B.K.M., K.A., M.S.F. and S.P. All authors have read and agreed to the published version of the manuscript.

Funding: Deep thanks and gratitude to the Researchers Supporting Project (RSP2023R351), King Saud University, Riyadh, Saudi Arabia for funding the research article. The authors would also like to extend the thanks and appreciation to the Indian Council of Social Science Research (ICSSR-MOST (Taiwan)/RP-1/2022-1C) for providing the financial support and Netaji Subhas Open University (AC/140/2021-22) for ensuring supportive research facilities to the research work.

Institutional Review Board Statement: Not Applicable.

Informed Consent Statement: Not Applicable.

Data Availability Statement: Data sharing not applicable. No new data were created or analyzed in this study. Data sharing is not applicable to this article.

Conflicts of Interest: The authors declare no conflict of interest.

Abbreviations

DEM	Digital Elevation Model
LULC	Land Use Land Cover
TWI	Topographic Wetness Index
NDVI	Normalized Difference Vegetation Index
MNDWI	Modified Normalized Difference Water Index
NDBI	Normalized Difference Built-Up Index
SPI	Standardized Precipitation Index
STI	Sediment Transport Index
AHP	Analytical Hierarchy Process
MCDM	Multi-Criteria Decision Making
GIS	Geographic Information System
F-AHP	Fuzzy Analytical Hierarchy Process
M.S.L.	Mean Sea Level
SODA	Solar Radiation Data
MERRA	Modern-Era Retrospective Analysis for Research and Applications
NASA	National Aeronautics and Space Administration
USGS	United States Geological Survey
NRSC	National Remote Sensing Centre
mm	Millimeter
SD	Standard Deviation
U statistics	Unbiased Statistics
NDWI	Normalized Difference Water Index
NDFI	Normalized Difference Flood Index
NDTI	Normalized Difference Turbidity Index
NDSI	Normalized Difference Soil Index
FVI	Flood Vulnerability Index
SWIR	Shortwave Infrared
CR	Consistency Ratio
CI	Consistency Index
RI	Random Index
CFVI	Composite Flood Vulnerability Index
CIb	Composite Ibrahim Index
SC	Scheduled Castes
ST	Scheduled Tribes
ANOVA	Analysis of Variance
ROC	Receiver Operating Characteristic
AUC	Area Under the ROC Curve
IDW	Inverse Distance Weight
SWOC	Strengths, Weaknesses, Opportunities, Challenges
SWOT	Strengths, Weaknesses, Opportunities, Threats
W1C1	Weakness 1, Challenge 1
O2S1	Opportunity 2, Strength 1
LMCI	Lower Mean Confidence Interval

UMCI	Upper Mean Confidence Interval
COV	Covariance
SRTM	Shuttle Radar Topographic Mission
ETM+	Enhanced Thematic Mapper Plus
LISSNIR	Linear Imaging Self ScanningNear Infrared
Std. Deviation	Standard Deviation
Df	Degree of Freedom
Sig.	Significance
VIF	Variance Inflation Factor

References

1. Nkwunonwo, U.C.; Whitworth, M.; Baily, B.; Inkpen, R. The development of a simplified model for urban flood risk mitigation in developing countries. In *Vulnerability, Uncertainty, and Risk: Quantification, Mitigation, and Management*; American Society of Civil Engineers: Reston, VA, USA, 2014; pp. 1116–1127. [CrossRef]
2. Bigi, V.; Comino, E.; Fontana, M.; Pezzoli, A.; Rosso, M. Flood vulnerability analysis in urban context: A socioeconomic sub-indicators overview. *Climate* **2021**, *9*, 12. [CrossRef]
3. Kundzewicz, Z.W.; Kanae, S.; Seneviratne, S.I.; Handmer, J.; Nicholls, N.; Peduzzi, P.; Sherstyukov, B. Flood risk and climate change: Global and regional perspectives. *Hydrol. Sci. J.* **2014**, *59*, 1–28. [CrossRef]
4. Zhou, Q.; Leng, G.; Huang, M. Impacts of future climate change on urban flood volumes in Hohhot in northern China: Benefits of climate change mitigation and adaptations. *Hydrol. Earth Syst. Sci.* **2018**, *22*, 305–316. [CrossRef]
5. Kashyap, S.; Mahanta, R. Vulnerability aspects of urban flooding: A review. *Indian J. Econ. Dev.* **2018**, *14*, 578–586. [CrossRef]
6. Gao, M.; Wang, Z.; Yang, H. Review of Urban Flood Resilience: Insights from Scientometric and Systematic Analysis. *Int. J. Environ. Res. Public Health.* **2022**, *19*, 8837. [CrossRef] [PubMed]
7. Chan, S.W.; Abid, S.K.; Sulaiman, N.; Nazir, U.; Azam, K.A. systematic review of the flood vulnerability using geographic information system. *Heliyon* **2022**, *8*, e09075. [CrossRef]
8. Gran Castro, J.A.; Ramos de Robles, S.L. Climate change and flood risk: Vulnerability assessment in an urban poor community in Mexico. *Environ. Urban.* **2019**, *31*, 75–92. [CrossRef]
9. Tingsanchali, T.; Promping, T. Comprehensive assessment of flood hazard, vulnerability, and flood risk at the household level in a municipality area: A case study of Nan Province, Thailand. *Water* **2022**, *14*, 161. [CrossRef]
10. Dewan, T.H. Societal impacts and vulnerability to floods in Bangladesh and Nepal. *Weather Clim. Extremes* **2015**, *7*, 36–42. [CrossRef]
11. National Disaster Management Authority. *National Disaster Management Guidelines: Management of Urban Flooding*; Government of India: New Delhi, India, 2010; pp. 1–158.
12. Prathipati, V.K.; CV, N.; Konatham, P. Inconsistency in the frequency of rainfall events in the Indian summer monsoon season. *Int. J. Climatol.* **2019**, *39*, 4907–4923. [CrossRef]
13. Vazhuthi, H.I.; Kumar, A. Causes and impacts of urban floods in Indian cities: A review. *Int. J. Emerg. Technol.* **2020**, *11*, 140–147.
14. Vignesh, K.S.; Anandakumar, I.; Ranjan, R.; Borah, D. Flood vulnerability assessment using an integrated approach of multi-criteria decision-making model and geospatial techniques. *Model. Earth Syst. Environ.* **2021**, *7*, 767–781. [CrossRef]
15. Haque, M.N.; Siddika, S.; Sresto, M.A.; Saroar, M.M.; Shabab, K.R. Geo-spatial analysis for flash flood susceptibility mapping in the North-East Haor (Wetland) Region in Bangladesh. *Earth Syst. Environ.* **2021**, *5*, 365–384. [CrossRef]
16. Vilasan, R.T.; Kapse, V.S. Evaluation of the prediction capability of AHP and F-AHP methods in flood susceptibility mapping of Ernakulam district (India). *Nat. Hazards.* **2022**, *112*, 1767–1793. [CrossRef]
17. Ramkar, P.; Yadav, S.M. Flood risk index in data-scarce river basins using the AHP and GIS approach. *Nat. Hazards.* **2021**, *109*, 1119–1140. [CrossRef]
18. Senan, C.P.; Ajin, R.S.; Danumah, J.H.; Costache, R.; Arabameri, A.; Rajaneesh, A.; Sajinkumar, K.S.; Kuriakose, S.L. Flood vulnerability of a few areas in the foothills of the Western Ghats: A comparison of AHP and F-AHP models. *Stoch. Environ. Res. Risk Assess.* **2022**, *37*, 527–556. [CrossRef]
19. Basu, T. An Analysis of the Unevenness of Intra Regional Development of Urban Space and Associated Vulnerabilities: A Study on Nabadwip Municipality in Nadia District, West Bengal, India. *IOSR J. Hum. Soc. Sci.* **2017**, *22*, 1–17.
20. Samal, N.R.; Roy, P.K.; Majumadar, M.; Bhattacharya, S.; Biswasroy, M. Six Years Major Historical Urban Floods in West Bengal State in India: Comparative Analysis Using Neuro-Genetic Model. *Am. J. Water Resour.* **2014**, *2*, 41–53. [CrossRef]
21. Idris, S.; Dharmasiri, L.M. Urban development and the increasing trend of flood risk in Gombe metropolis, Nigeria. *Int. J. Sci. Res.* **2015**, *5*, 500–504.
22. Wang, C.; Du, S.; Wen, J.; Zhang, M.; Gu, H.; Shi, Y.; Xu, H. Analyzing explanatory factors of urban pluvial floods in Shanghai using geographically weighted regression. *Stoch. Environ. Res. Risk Assess.* **2017**, *31*, 1777–1790. [CrossRef]
23. Bezboruah, K.; Sattler, M.; Bhatt, A. Flooded Cities: A Comparative Analysis of Flood Management Policies in Indian states. *Int. J. Water Gov.* **2021**, *17*, 8. [CrossRef]
24. Zhu, W.; Cao, Z.; Luo, P.; Tang, Z.; Zhang, Y.; Hu, M.; He, B. Urban Flood-Related Remote Sensing: Research Trends, Gaps and Opportunities. *Remote Sens.* **2022**, *14*, 5505. [CrossRef]

25. Sarmah, T.; Das, S.; Narendr, A.; Aithal, B.H. Assessing human vulnerability to urban flood hazard using the analytic hierarchy process and geographic information system. *Int. J. Disaster Risk Reduct.* **2020**, *50*, 101659. [CrossRef]
26. Rafiq, F.; Ahmed, S.; Ahmad, S.; Khan, A.A. Urban floods in India. *Int. J. Sci. Eng. Res.* **2016**, *7*, 721–734.
27. Jha, C.V.; Bairagya, H. Flood and flood plains of West Bengal, India: A comparative analysis. *Revista Geoaraguaia* **2013**, *3*, 1–10.
28. Sanyal, J.; Lu, X.X. Remote sensing and GIS-based flood vulnerability assessment of human settlements: A case study of Gangetic West Bengal, India. *Hydrol. Process* **2005**, *19*, 3699–3716. [CrossRef]
29. Sanyal, J.; Lu, X.X. GIS-based flood hazard mapping at different administrative scales: A case study in Gangetic West Bengal, India. *Singap. J. Trop. Geogr.* **2006**, *27*, 207–220. [CrossRef]
30. Bhattacharjee, K.; Behera, B. Determinants of household vulnerability and adaptation to floods: Empirical evidence from the Indian State of West Bengal. *Int. J. Disaster Risk Reduct.* **2018**, *31*, 758–769. [CrossRef]
31. Rumbach, A. At the roots of urban disasters: Planning and uneven geographies of risk in Kolkata, India. *J. Urban Aff.* **2017**, *39*, 783–799. [CrossRef]
32. Roy, U. Impact on the life of common people for the floods in coloneal period (1770 AD-1900 AD) & recent time (1995 AD-2016 AD): A case study of Nadia district, West Bengal. *J. Emerg. Technol. Innov. Res.* **2019**, *6*, 216–223.
33. Khatun, R. Focus on better planning for flood disaster recovery in West Bengal: A geographical analysis. *Int. J. Soc. Sci. Econ. Res.* **2018**, *3*, 3673–3691.
34. Mallick, S. Identification of fluvio-geomorphological changes and bank line shifting of river Bhagirathi-Hugli using remote sensing technique in and around of Mayapur Nabadwip area, West Bengal. *Int. J. Sci. Res.* **2016**, *5*, 1130–1134.
35. Census of India. *District Census Handbook Nadia, Village and Town Wise Primary Census Abstract (PCA)*; Directorate of Census Operations: West Bengal, India, 2011; Series 20, Part-XII A and B, pp. 1–464. Available online: https://censusindia.gov.in/pca/ (accessed on 19 March 2022).
36. NASA (National Aeronautics and Space Administration). Shuttle Radar Topographic Mission (SRTM). EARTHDATA. USA.gov. 2000. Available online: https://www2.jpl.nasa.gov/srtm/ (accessed on 30 August 2022).
37. NRSC (National Remote Sensing Centre). *Cartosat-1*; Government of India: New Delhi, India, 2015. Available online: https://bhuvan.nrsc.gov.in/home/index.php (accessed on 30 August 2022).
38. USGS (United States Geological Survey). *Landsat Data Access. Department of Interior*; United States Geological Survey: Washington, DC, USA, 2000. Available online: https://earthexplorer.usgs.gov/ (accessed on 30 August 2022).
39. NRSC (National Remote Sensing Centre). *Resourcesat-1/Resoursat-2: LISS-III*; Government of India: New Delhi, India, 2015. Available online: https://bhuvan.nrsc.gov.in/home/index.php (accessed on 30 August 2022).
40. India Meteorological Department. *Climatological Table*; Ministry of Earth Sciences, Government of India: New Delhi, India, 2000.
41. India Meteorological Department. *Climatological Table*; Ministry of Earth Sciences, Government of India: New Delhi, India, 2015.
42. Global Modeling and Assimilation Office (GMAO). *MERRA-2 Day and Month-wise Rainfall Data of Selected Coordinate Points in West Bengal, India*; Goddard Earth Sciences Data and Information Services Center (GES DISC): Greenbelt, MD, USA, 2015. [CrossRef]
43. European Commission. Copernicus European Drought Observatory (EDO). 2020. Available online: https://edo.jrc.ec.europa.eu (accessed on 1 August 2022).
44. Santos, E.B.; de Freitas, E.D.; Rafee, S.A.; Fujita, T.; Rudke, A.P.; Martins, L.D.; Ferreira de Souza, R.A.; Martins, J.A. Spatio-temporal variability of wet and drought events in the Paraná River basin—Brazil and its association with the El Niño—Southern oscillation phenomenon. *Int. J. Climatol.* **2021**, *41*, 4879–4897. [CrossRef]
45. Li, R.; Cheng, L.; Ding, Y.; Chen, Y.; Khorasani, K. Spatial and temporal variability analysis in rainfall using standardized precipitation index for the Fuhe Basin, China. In Proceedings of the Intelligent Computing for Sustainable Energy and Environment: Second International Conference, Shanghai, China, 12–13 September 2012; Springer: Berlin/Heidelberg, Germany, 2013; pp. 451–459.
46. Guerreiro, M.J.; Lajinha, T.; Abreu, I. *Flood Analysis with the Standardized Precipitation Index (SPI)*; Edições Universidade Fernando Pessoa: Porto, Portugal, 2007; Volume 4, pp. 1–7.
47. Olanrewaju, C.C.; Reddy, M. Assessment and prediction of flood hazards using standardized precipitation index—A case study of eThekwini metropolitan area. *J. Flood Risk Manag.* **2022**, *15*, e12788. [CrossRef]
48. Seiler, R.A.; Hayes, M.; Bressan, L. Using the standardized precipitation index for flood risk monitoring. *Int. J. Climatol.* **2002**, *22*, 1365–1376. [CrossRef]
49. Edwards, D.C.; McKee, T.B. *Characteristics of 20th Century Drought in the United States at Multiple Time Scales*; Climatology Report No. 97–2; Colorado State University: Fort Collins, CO, USA, 1997; pp. 1–155.
50. Naresh Kumar, M.; Murthy, C.S.; Sesha Sai, M.V.; Roy, P.S. On the use of Standardized Precipitation Index (SPI) for drought intensity assessment. *Meteorol. Appl.* **2009**, *16*, 381–389. [CrossRef]
51. Abromowitz, M.; Stegun, I.A. *Handbook of Mathematical Functions*; Applied Mathematics Series; National Bureau of Standards: Washington, DC, USA, 1965.
52. McKee, T.B.; Doesken, N.J.; Kleist, J. The relationship of drought frequency and duration to time scales. In Proceedings of the 8th Conference on Applied Climatology, Anaheim, CA, USA, 17–22 January 1993; Volume 17, pp. 179–183. Available online: https://climate.colostate.edu/pdfs/relationshipofdroughtfrequency.pdf (accessed on 1 August 2022).
53. Smith, K.G. Standards for grading texture of erosional topography. *Am. J. Sci.* **1950**, *248*, 655–668. [CrossRef]

54. Schumm, S.A. Evolution of drainage systems and slopes in badlands at Perth Amboy, New Jersey. *Geol. Soc. Am. Bull.* **1956**, *67*, 597–646.
55. Wentworth, C.K. A simplified method of determining the average slope of land surfaces. *Am. J. Sci.* **1930**, *5*, 184–194. [CrossRef]
56. Lemenkova, P. Flow Direction and Length Determined by ArcGIS Spatial Analyst and Terrain Elevation Data Sets. In Proceedings of the Conference 'Priority Directions of the Development of Young Research Farmers in Modern Science', 25th Anniversary of Caspian Research Institute of Arid Agriculture RAAS, Moscow, Russia, 11–13 May 2016; Shherbakova, N.A., Bondarenko, A.N., Eds.; PNIIAZ: Moscow, Russia, 2016; pp. 579–583.
57. Martz, L.W.; Garbrecht, J. Numerical definition of drainage network and subcatchment areas from digital elevation models. *Comput. Geosci.* **1992**, *18*, 747–761. [CrossRef]
58. Rouse, J.W.; Haas, R.H.; Schell, J.A.; Deering, D.W. Paper a 20. In *Third Earth Resources Technology Satellite-1 Symposium: Section AB*; Technical Presentations; National Aeronautics and Space Administration: Washington, DC, USA, 1973; Volume 1, p. 309.
59. McFeeters, S.K. The use of the Normalized Difference Water Index (NDWI) in the delineation of open water features. *Int. J. Remote Sens.* **1996**, *17*, 1425–1432. [CrossRef]
60. Xu, H. A study on information extraction of water body with the modified normalized difference water index (MNDWI). *J. Remote Sens.* **2005**, *9*, 589–595.
61. Zha, Y.; Gao, J.; Ni, S. Use of normalized difference built-up index in automatically mapping urban areas from TM imagery. *Int. J. Remote Sens.* **2003**, *24*, 583–594. [CrossRef]
62. Elhag, M.; Gitas, I.; Othman, A.; Bahrawi, J.; Gikas, P. Assessment of water quality parameters using temporal remote sensing spectral reflectance in arid environments, Saudi Arabia. *Water* **2019**, *11*, 556. [CrossRef]
63. Lacaux, J.P.; Tourre, Y.M.; Vignolles, C.; Ndione, J.A.; Lafaye, M. Classification of ponds from high-spatial resolution remote sensing: Application to Rift Valley Fever epidemics in Senegal. *Remote Sens. Environ.* **2007**, *106*, 66–74. [CrossRef]
64. Deng, Y.; Wu, C.; Li, M.; Chen, R. RNDSI: A ratio normalized difference soil index for remote sensing of urban/suburban environments. *Int. J. Appl. Earth Obs. Geoinf.* **2015**, *39*, 40–48. [CrossRef]
65. Wan, K.M.; Billa, L. Post-flood land use damage estimation using improved Normalized Difference Flood Index (NDFI3) on Landsat 8 datasets: December 2014 floods, Kelantan, Malaysia. *Arab. J. Geosci.* **2018**, *11*, 434. [CrossRef]
66. Boschetti, M.; Nutini, F.; Manfron, G.; Brivio, P.A.; Nelson, A. Comparative analysis of normalised difference spectral indices derived from MODIS for detecting surface water in flooded rice cropping systems. *PLoS ONE* **2014**, *9*, e88741. [CrossRef]
67. Cian, F.; Marconcini, M.; Ceccato, P. Normalized Difference Flood Index for rapid flood mapping: Taking advantage of EO big data. *Remote Sens. Environ.* **2018**, *209*, 712–730. [CrossRef]
68. Deepak, S.; Rajan, G.; Jairaj, P.G. Geospatial approach for assessment of vulnerability to flood in local self-governments. *Geoenviron. Dis.* **2020**, *7*, 1–19. [CrossRef]
69. Taromideh, F.; Fazloula, R.; Choubin, B.; Emadi, A.; Berndtsson, R. Urban flood-risk assessment: Integration of decision-making and machine learning. *Sustainability* **2022**, *14*, 4483. [CrossRef]
70. Saaty, R.W. The analytic hierarchy process—What it is and how it is used. *Math. Model* **1987**, *9*, 161–176. [CrossRef]
71. Bozdağ, A.; Yavuz, F.; Günay, A.S. AHP and GIS based land suitability analysis for Cihanbeyli (Turkey) County. *Environ. Earth Sci.* **2016**, *75*, 813. [CrossRef]
72. Saaty, T.L. A scaling method for priorities in hierarchical structures. *J. Math. Psychol.* **1977**, *15*, 234–281. [CrossRef]
73. Saaty, T.L. *The Analytic Hierarchy Process*; Agricultural Economics Review; McGraw Hill: New York, NY, USA, 1980; Volume 70.
74. Abu Dabous, S.; Alkass, S. Decision support method for multi-criteria selection of bridge rehabilitation strategy. *Constr. Manag. Econ.* **2008**, *26*, 883–893. [CrossRef]
75. Bhushan, N.; Rai, K. *Strategic Decision Making: Applying the Analytic Hierarchy Process*; Springer: London, UK, 2004; pp. 1–170.
76. Ibrahim, M. *Ibrahim Index of African Governance*; Data Report; Mo Ibrahim Foundation: London, UK, 2012.
77. Gisselquist, R.M. *Evaluating Governance Indexes: Critical and Less Critical Questions*; WIDER Working Paper Series wp-2013-068; World Institute for Development Economic Research (UNU-WIDER): Helsinki, Finland, 2013.
78. Uyanık, G.K.; Güler, N. A study on multiple linear regression analysis. *Procedia Soc. Behav. Sci.* **2013**, *106*, 234–240. [CrossRef]
79. Pearson, K. *VII. Mathematical Contributions to the Theory of Evolution—III. Regression, Heredity, and Panmixia*; University College London: London, UK, 1896; Volume 187, pp. 253–318. Available online: http://rsta.royalsocietypublishing.org/content/187/253.full.pdf (accessed on 1 August 2022)Containing Papers of a Mathematical or Physical Character.
80. Pearson, K. On certain errors with regard to multiple correlation occasionally made by those who have not adequately studied this subject. *Biometrika* **1914**, *10*, 181–187. Available online: http://www.jstor.org/stable/2331747 (accessed on 1 August 2022).
81. Durbin, J.; Watson, G.S. Testing For Serial Correlation in Least Squares Regression. III. *Biometrika* **1971**, *58*, 1–19. [CrossRef]
82. Farebrother, R.W. The Durbin-Watson test for serial correlation when there is no intercept in the regression. *Econometrica* **1980**, *48*, 1553–1563. [CrossRef]
83. Holt, W.; Refenes, P. The Durbin-Watson test for neural regression models. In *Risk Measurement, Econometrics and Neural Networks: Selected Articles of the 6th Econometric-Workshop in Karlsruhe, Germany*; Physica-Verlag HD: Heidelberg, Germany, 1998; pp. 57–68. [CrossRef]
84. Fisher, R.A. *Statistical Methods for Research Workers*; Oliver and Boyd London and Edinburgh (§4 and §42 (Ex. 41) Reproduced; Springer: Berlin/Heidelberg, Germany, 1934.

85. Welch, B.L. The generalization of 'student's' problem when several different population variances are involved. *Biometrika* **1947**, *34*, 28–35. [CrossRef] [PubMed]
86. Nam, B.H.; D'Agostino, R.B. Discrimination index, the area under the ROC curve. In *Goodness-of-Fit Tests and Model Validity*; Huber-Carol, C., Balakrishnan, N., Nikulin, M.S., Mesbah, M., Eds.; Birkhäuser Boston: Boston, MA, USA, 2002; pp. 267–279.
87. Grimnes, S.; Martinsen, Ø.G. *Bioimpedance and Bioelectricity Basics*; Elsevier: Amsterdam, The Netherlands, 2015; pp. 329–404. [CrossRef]
88. Khosravi, K.; Pourghasemi, H.R.; Chapi, K.; Bahri, M. Flash flood susceptibility analysis and its mapping using different bivariate models in Iran: A comparison between Shannon's entropy, statistical index, and weighting factor models. *Environ. Monit. Assess.* **2016**, *188*, 1–21. [CrossRef] [PubMed]
89. Farhadi, H.; Najafzadeh, M. Flood risk mapping by remote sensing data and random forest technique. *Water* **2021**, *13*, 3115. [CrossRef]
90. Saha, A.K.; Agrawal, S. Mapping and assessment of flood risk in Prayagraj district, India: A GIS and remote sensing study. *Nanotechnol. Environ. Eng.* **2020**, *5*, 1–18. [CrossRef]
91. Irrigation and Waterways Directorate. *Annual Flood Report 2000*; Government of West Bengal: West Bengal, India, 2000; pp. 1–17.
92. Irrigation and Waterways Directorate. *Annual Flood Report for the Year 2015*; Advance Planning, Project Evaluation & Monitoring Cell; Government of West Bengal: West Bengal, India, 2015; pp. 1–57.
93. Binns, A.D. Flood mitigation measures in an era of evolving flood risk. *J. Flood Risk Manag.* **2020**, *13*, e12659. [CrossRef]
94. van Doorn-Hoekveld, W.; Groothuijse, F. Analysis of the strengths and weaknesses of Dutch water storage areas as a legal instrument for flood-risk prevention. *J. Eur. Environ. Plan Law* **2017**, *14*, 76–97. [CrossRef]
95. Grama, V.; Avanzi, A.; Nistor-Lopatenco, L. SWOT principle in flood risk management. *J. Eng. Sci.* **2021**, *15*, 125–137. [CrossRef]
96. Noorhashirin, H.; Juni, M.H. Assessing Malaysian disaster preparedness for flood. *Int. J. Public Health Clin. Sci.* **2016**, *3*, 1–5.